Quantum Imaging Technologies: Quantum Laser Radar & Entanglement Utilizing Complex Pump Mode Patterns

Prem Kumar and Geraldo A. Barbosa

Center for Photonic Communication and Computing
ECE Department, Northwestern University, Evanston, IL 60208-3118
Tel: (847) 491-4128; Fax: (847) 467-5319
E-mails: kumarp@northwestern.edu; g-barbosa@northwestern.edu

Support: **U. S. Army Research Office Multidisciplinary University Research Initiative Grant No W911NF-05-1-0197**

Northwestern Team's SOW

Quantum Laser Radar: (System)

We will develop quantum imaging techniques specially suited to enhancing the sensitivity and resolution of laser radar. Specific topics to be studied include the use of phase-sensitive amplification as a noiseless preamplification process for enhancing the sensitivity of radar receivers and the use of specially prepared illumination schemes that will enhance system sensitivity. All measurements will be quantified in a manner that allows characterization of the systems aspects of laser radar. (Collaboration with MIT)

Entanglement Utilizing Complex Pump Mode Patterns: (Technology)

We will develop a source of entangled photons based on the orbital angular momentum of light. We will measure and quantify the degree of spatial correlation of this entangled state of light. We will develop new methods to measure the orbital angular momentum of the entangled photons and quantum imaging applications including a quantum motion sensor. (Collaboration with University of Rochester)

Quantum-Limited Sensitivity of Imaging

Amplitude Objects:

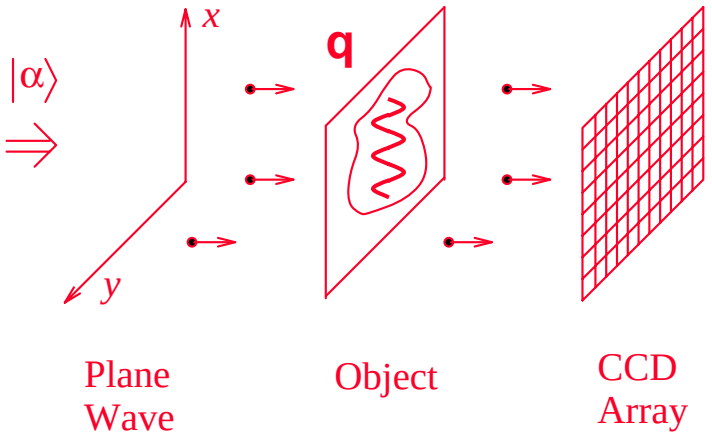

Spatially white shot noise $\propto \frac{1}{|\alpha|^2}$

Phase Objects:

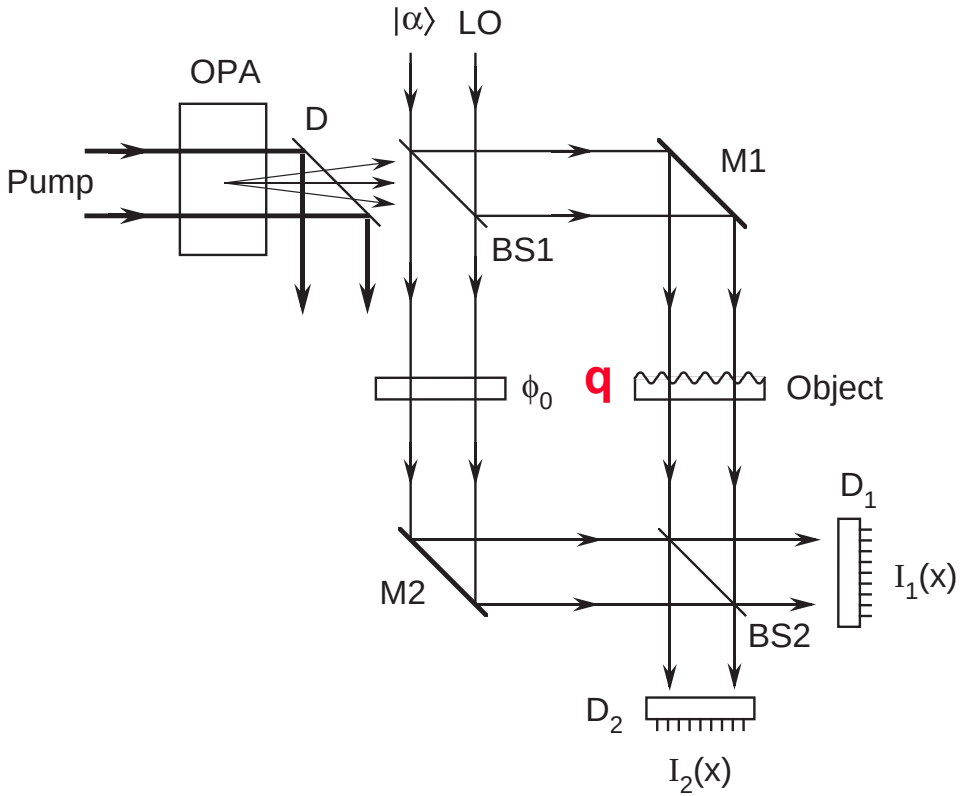

- M. I. Kolobov and P. Kumar, "Sub-shot–noise microscopy: Imaging of faint phase objects with squeezed light," Opt. Lett. **18**, 849 (1993).
- P. Kumar and M. I. Kolobov, "Four-Wave Mixing as a Source for spatially broadband squeezed light," Opt. Commun. **104**, 374 (1994).

Setup for Parametric Image Amplification

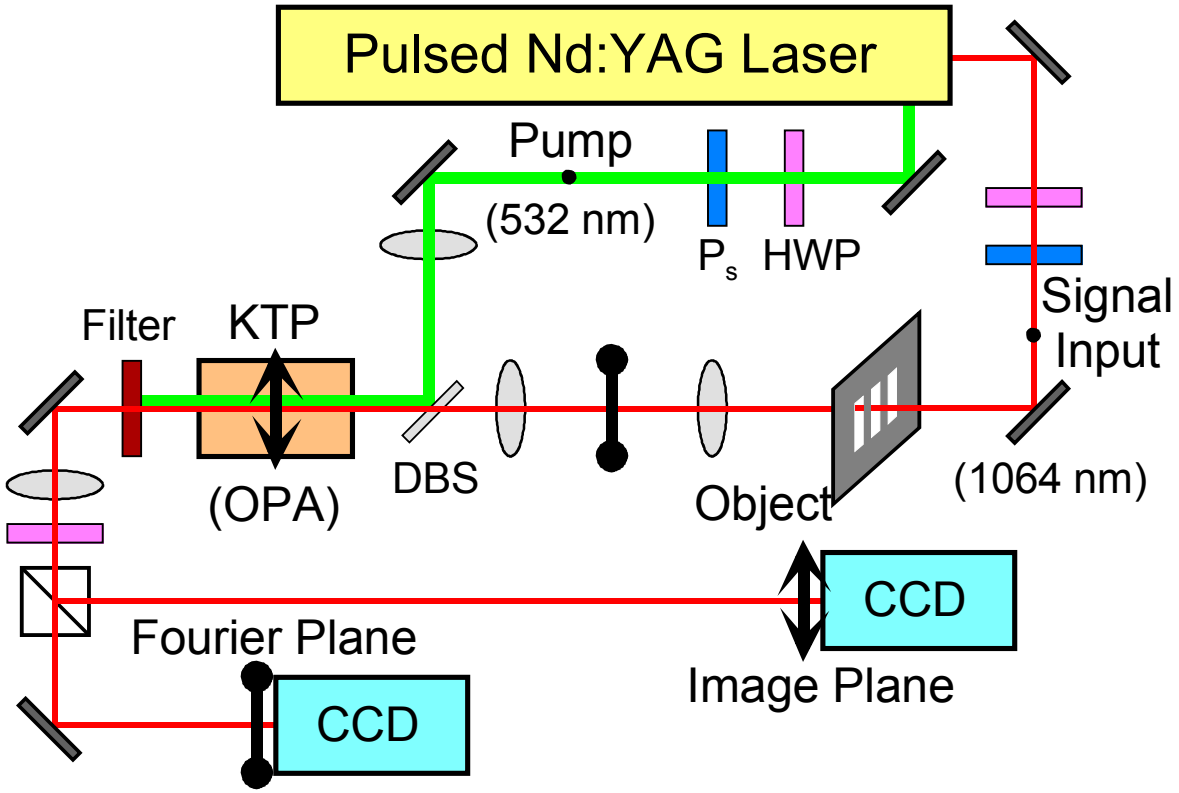

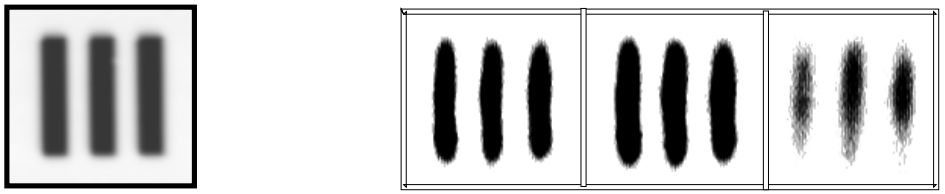

Object Plane **Image Plane**

Parametrically Amplified Images

Object Plane

16 lines/mm

Image Plane

bare signal | amplified signal | idler

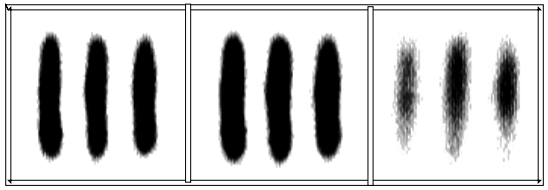

Fourier Plane

Bare Signal

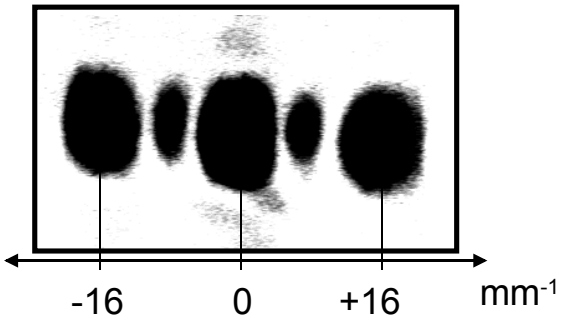

Amplified Signal (Low-Pass OPA)

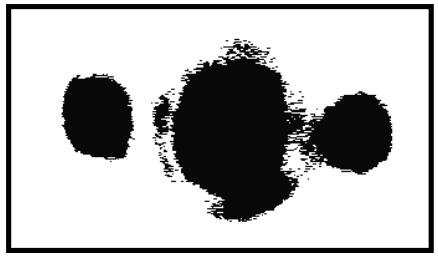

USAF Test Pattern

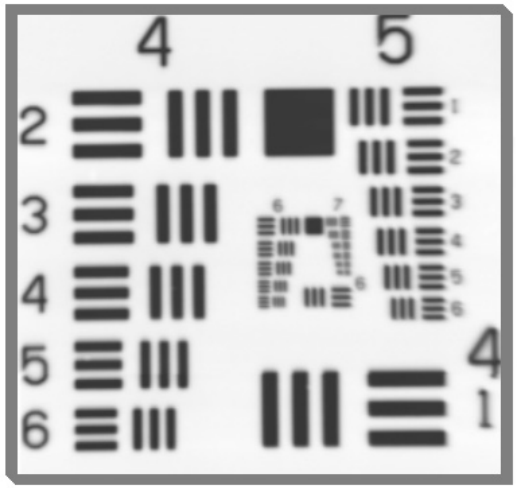

Amplified Signal (Band-Pass OPA)

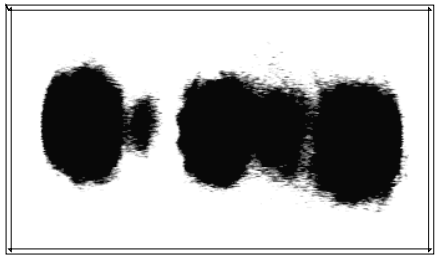

Correlated Twin Beams

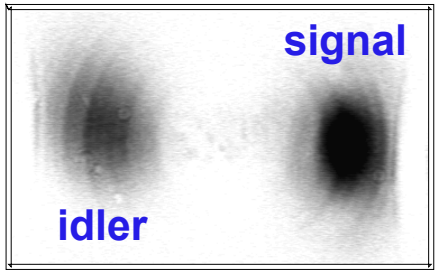

Setup for Noise Measurements

Input Signal

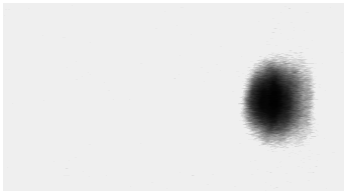

Amplified Signal

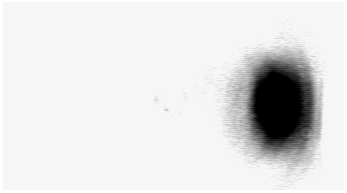

Idler

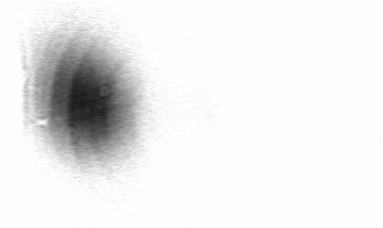

Amplified Signal / Idler

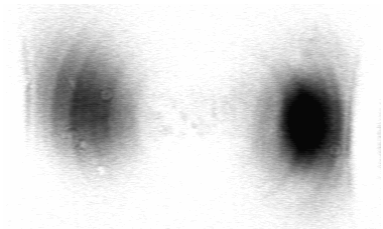

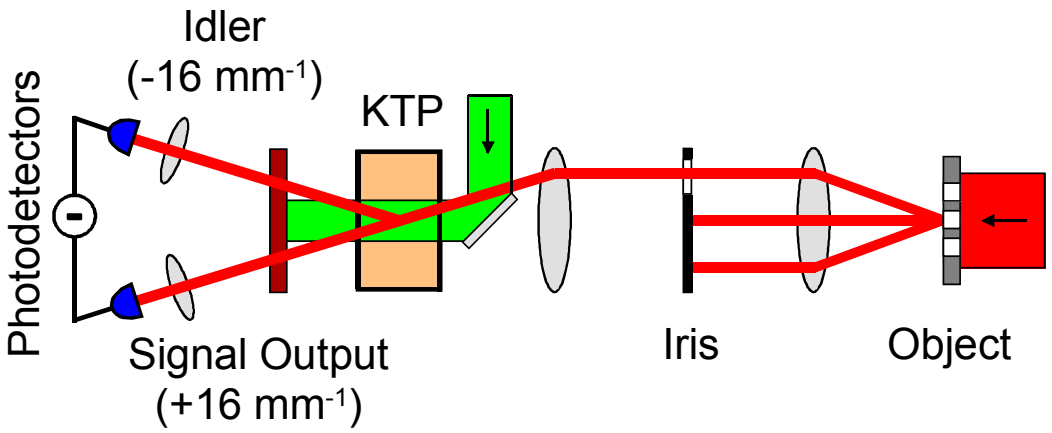

Top View of the Layout

[Images for Noise Measurements]

Spatially Broadband OPA Theory

Parametric gain: phase-insensitive gain $G_{PIA} = |\mu|^2$

phase-sensitive gain $G_{PSA} = 2G_{PIA} - 1 + 2\sqrt{G_{PIA}(G_{PIA}-1)}$

Twin beam noise reduction: $R = \frac{\eta}{|\mu|^2 + |\nu|^2} + 1 - \eta$

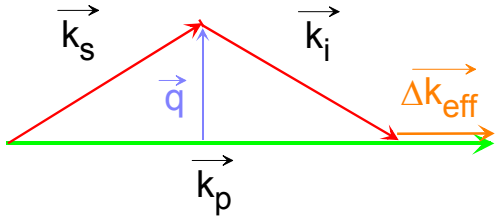

$$\mu = [\cosh(hl) + \frac{i\Delta k_{eff}}{2h}\sinh(hl)]\exp(-\frac{i\Delta k_{eff} l}{2})$$

η = quantum efficiency

$$\nu = -\frac{ig}{2h}\sinh(hl)\exp(-\frac{i\Delta k_{eff} l}{2})$$

$$h = \frac{1}{2}\sqrt{|g|^2 - \Delta k_{eff}{}^2}$$

$g \propto$ (pump intensity)$^{1/2}$

$$\Delta k_{eff} = k_p - k_s - k_i + \frac{q^2}{2}(\frac{1}{k_s} + \frac{1}{k_i})$$

l = length of nonlinear crystal

ref.: A. Gavrielides, P. Peterson, and D. Cardimona, J. Appl. Phys. **62**, 2640 (1987).

Twin-Beams Noise Reduction

vs. OPA Gain

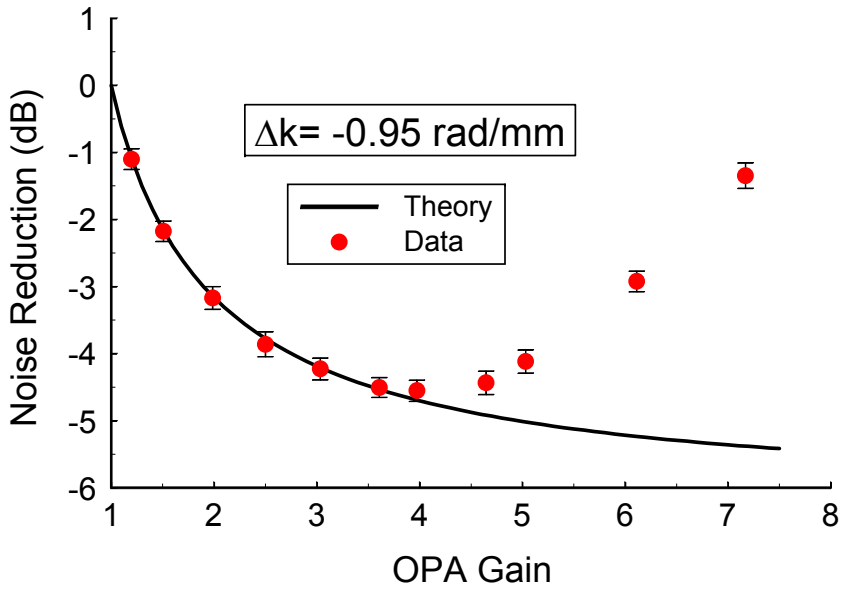

vs. Δk

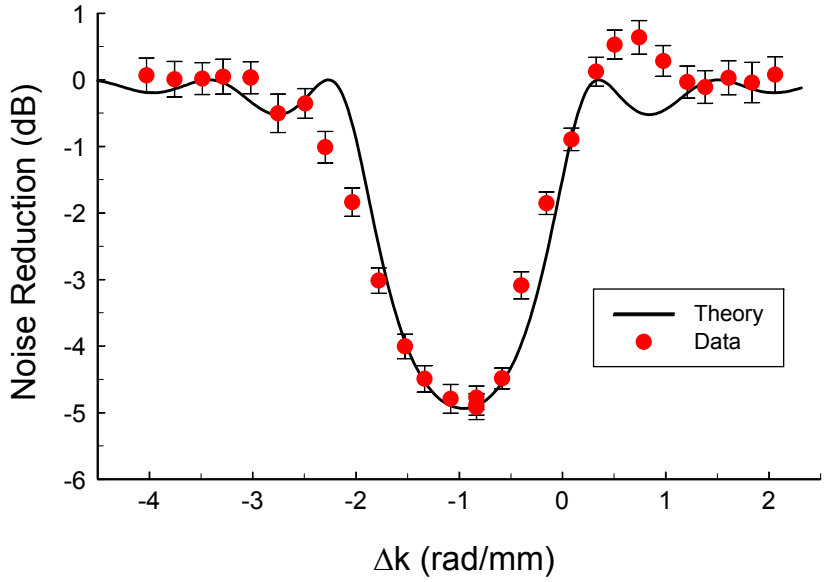

M. L. Marable, S-K. Choi, and P. Kumar, *Optics Express* **2**, 84–92 (1998).

Amplification of Coherent Light Input

$\sigma_{out}^2 = (2g - 1)\,\sigma_{in}^2$

$E = X + i\,Y$

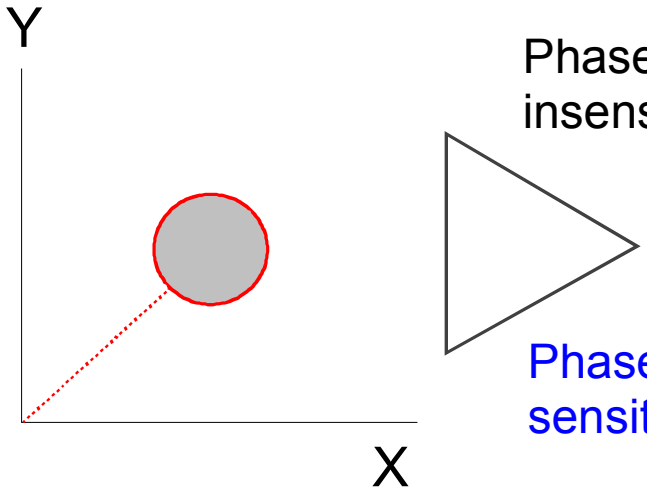

Phase-insensitive

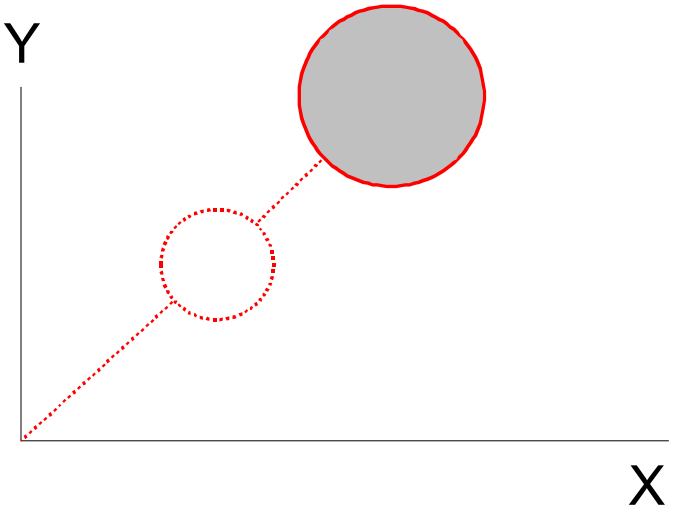

Phase-sensitive

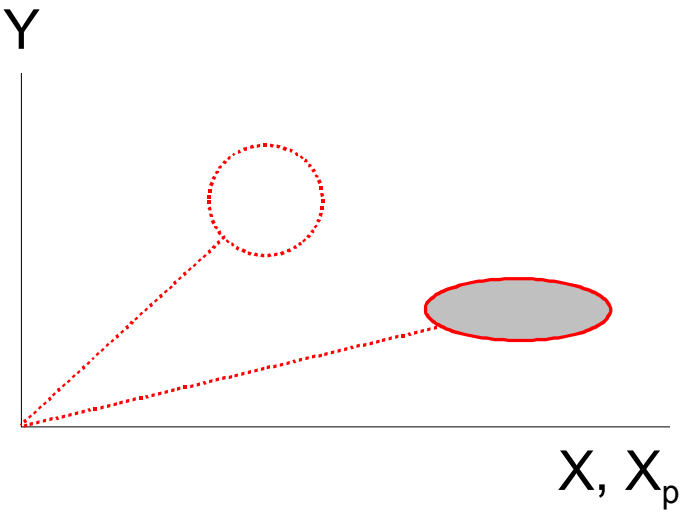

$\sigma_X^2 = G\,\sigma_{in}^2$

$\sigma_Y^2 = G^{-1}\,\sigma_{in}^2$

Layout for Noiseless Image Amplification

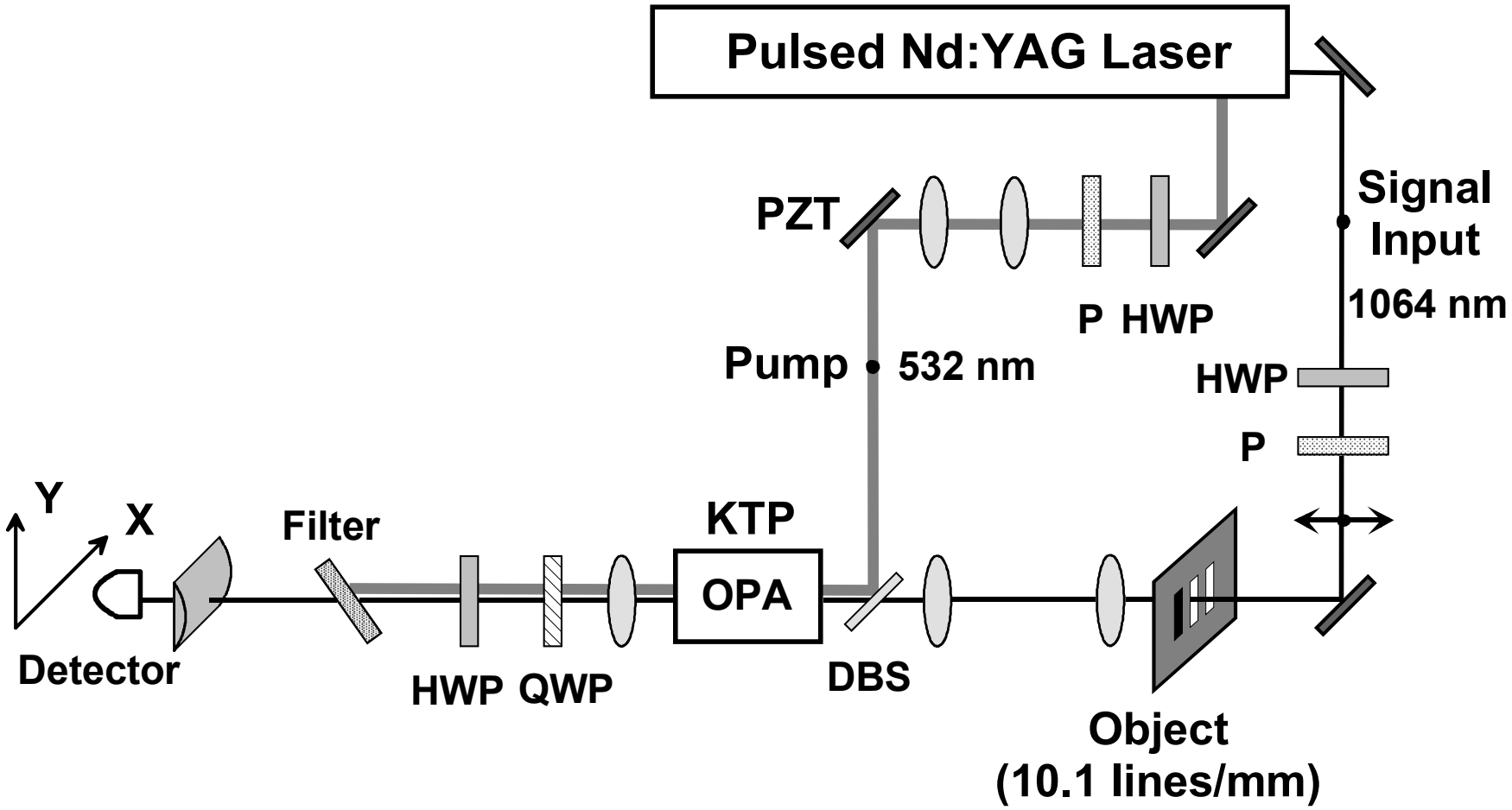

S.-K. Choi, M. Vasilyev, and P. Kumar, *Phys. Rev. Lett.* **83**, 1938 –1941 (1999).

Spatial Profiles of 1-d Image

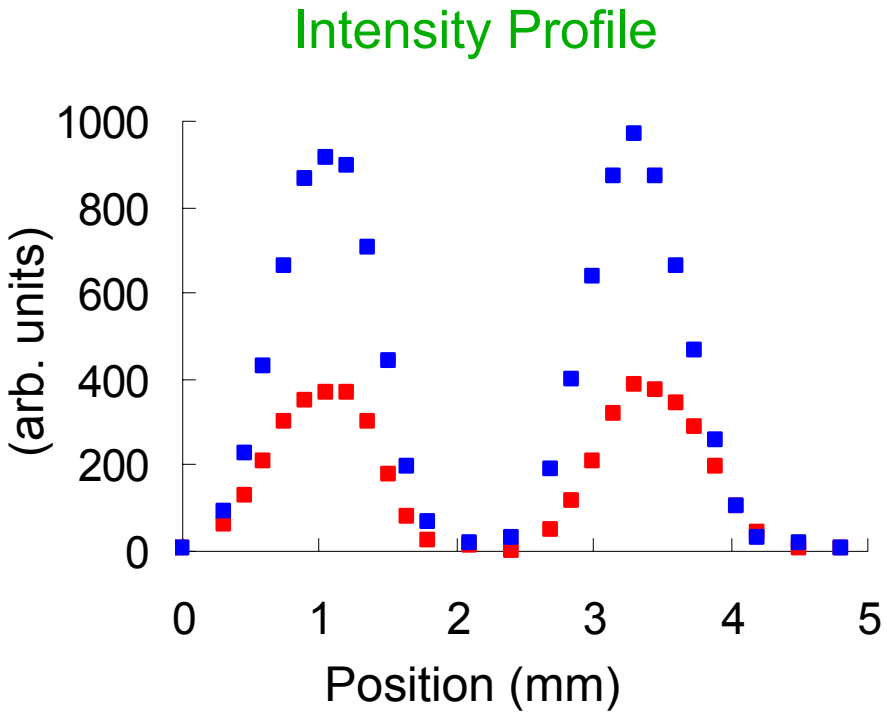

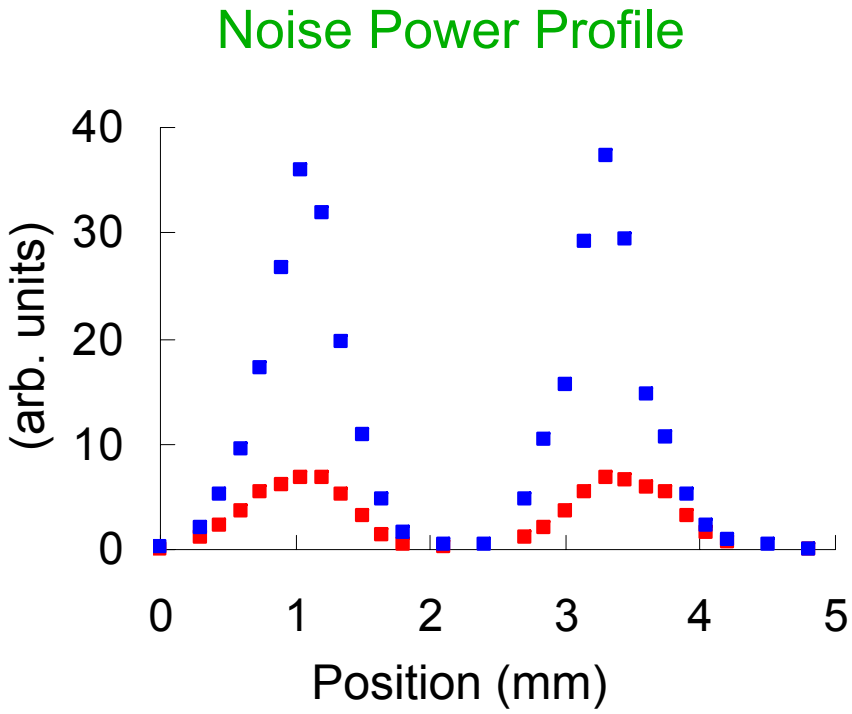

- 2-slit object magnified x24 and then compressed in one dimension
- Spatial profiles scanned by photodetector in horizontal direction
- Red squares – bare profile; Blue squares – PSA profile
- 3.25 mm KTP crystal

S.-K. Choi, M. Vasilyev, and P. Kumar, *Phys. Rev. Lett.* **83**, 1938 –1941 (1999).

Amplifier Noise Figure

DC gain vs. 27 MHz gain

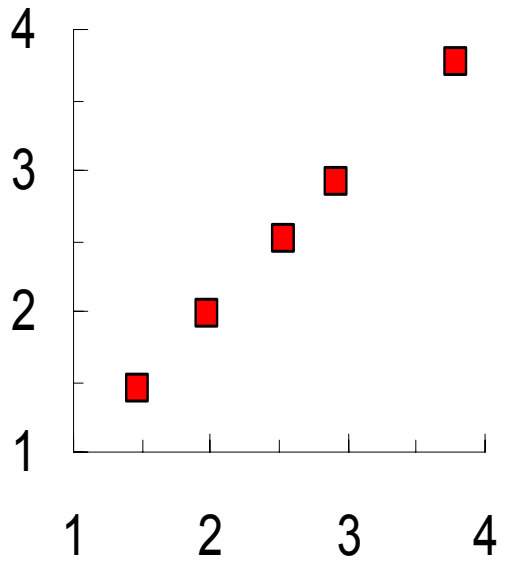

- Experimental $NF_{amp+loss}$

$$= \frac{1}{\eta}\frac{(27\text{ MHz gain})}{(\text{DC gain})^2}$$

- $NF_{amp+loss} = NF_{amp} + (1-\eta)/(\eta G)$

- PIA $SNR_{out} = \dfrac{\eta G}{2\eta G + 1 - 2\eta} SNR_{in}$

$$NF_{amp+loss} = 2 + \frac{1}{\eta G} - \frac{2}{G}$$

- PSA $SNR_{out} = \dfrac{\eta G}{\eta G + 1 - \eta} SNR_{in}$

$$NF_{amp+loss} = 1 + \frac{1-\eta}{\eta G}$$

PSA gain G = 2.5-2.6 Quantum eff. η = 0.82

$NF_{amp+loss}$	3.25mm KTP	5.21mm KTP
PSA Exp. @ peaks	1.05 ± 0.1 0.2 ± 0.6 dB	1.10 ± 0.1 0.4 ± 0.5 dB
PSA Theory	1.1 0.4 dB	1.1 0.4 dB
PIA Theory	1.7 2.3 dB	1.7 2.3 dB

Conclusions from Past Work

Quantum Noise Correlations In Image Amplification

- Observation of quantum noise reduction in non-collinear twin beams
  5 dB below the shot-noise level
- Good agreement with theory of spatially-broadband OPA
- Bandpass OPA selects spatial frequency for amplification

Noiseless Image Amplification

- Spatially broadband noiseless image amplification
  PSA gain $\cong$ 2.5 and $NF_{amp} \cong 0$ dB at peaks of amplified 2-slit image
- Improvement of detected SNR due to pre-amplification before loss
  $NF_{amp+loss} \cong$ 0.2-0.4 dB $<$ $NF_{bare+loss} \cong$ 0.9 dB

Experimental investigation of a frequency non-degenerate phase-sensitive parametric amplifier

Renyong Tang, Preetpaul Devgan, Jacob Lasri, Vladimir Grigoryan and Prem Kumar

This work was supported by the National Science Foundation under Grants: ANI-0123495, and the IGERT DGE-9987577.

Four-Wave-Mixing Process in Optical Fibers

$$\begin{cases} \dfrac{dP_p}{dz} = -\alpha P_p - 4\gamma (P_p P_s P_a)^{1/2} \sin\theta \\ \dfrac{dP_s}{dz} = -\alpha P_s + 2\gamma (P_p^{\,2} P_s P_a)^{1/2} \sin\theta \\ \dfrac{dP_a}{dz} = -\alpha P_a + 2\gamma (P_p^{\,2} P_s P_a)^{1/2} \sin\theta \\ \dfrac{d\theta}{dz} = \Delta\beta + \gamma\{ 2P_p - P_s - P_a + [(P_p^{\,2} P_s / P_a)^{1/2} \\ \qquad + (P_p^{\,2} P_a / P_s)^{1/2} - 4(P_s P_a)^{1/2}]\cos\theta\}, \\ \theta = \Delta\beta\, z + \phi_s(z) + \phi_a(z) - 2\,\phi_p(z) \end{cases}$$

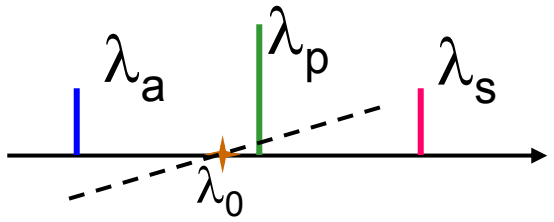

s: stokes, a: anti-stokes
p: pump, P: power
ϕ: phase, α: loss coefficient
β: propagation constant

$$\Delta\beta = \beta_s + \beta_a - 2\,\beta_p$$

$\kappa = \Delta\beta + 2\,\kappa\, P_p$,
$g = [(\gamma P_p)^2 - (\kappa/2)^2]^{1/2}$

$\eta = (P_a(0)/P_s(0))^{1/2}$

$$G = 1 + \{1 + \frac{4\gamma^2 P_p^{\,2}\eta^2 + \kappa^2 + 4\gamma\kappa P_p \eta\cos(\theta)}{4g^2}\}\sinh^2(gL) + \frac{\gamma P_p \eta \sin(\theta)}{g}\sinh(2gL)$$

Ideally, PSA provides 6 dB more gain than PIA does.

FOPA-PSA: $G_{max} \sim \{\exp(gL)\}^2$, FOPA-PSA: $G_{max} \sim \{\exp(gL)\}^2/4$

Experimental Setup

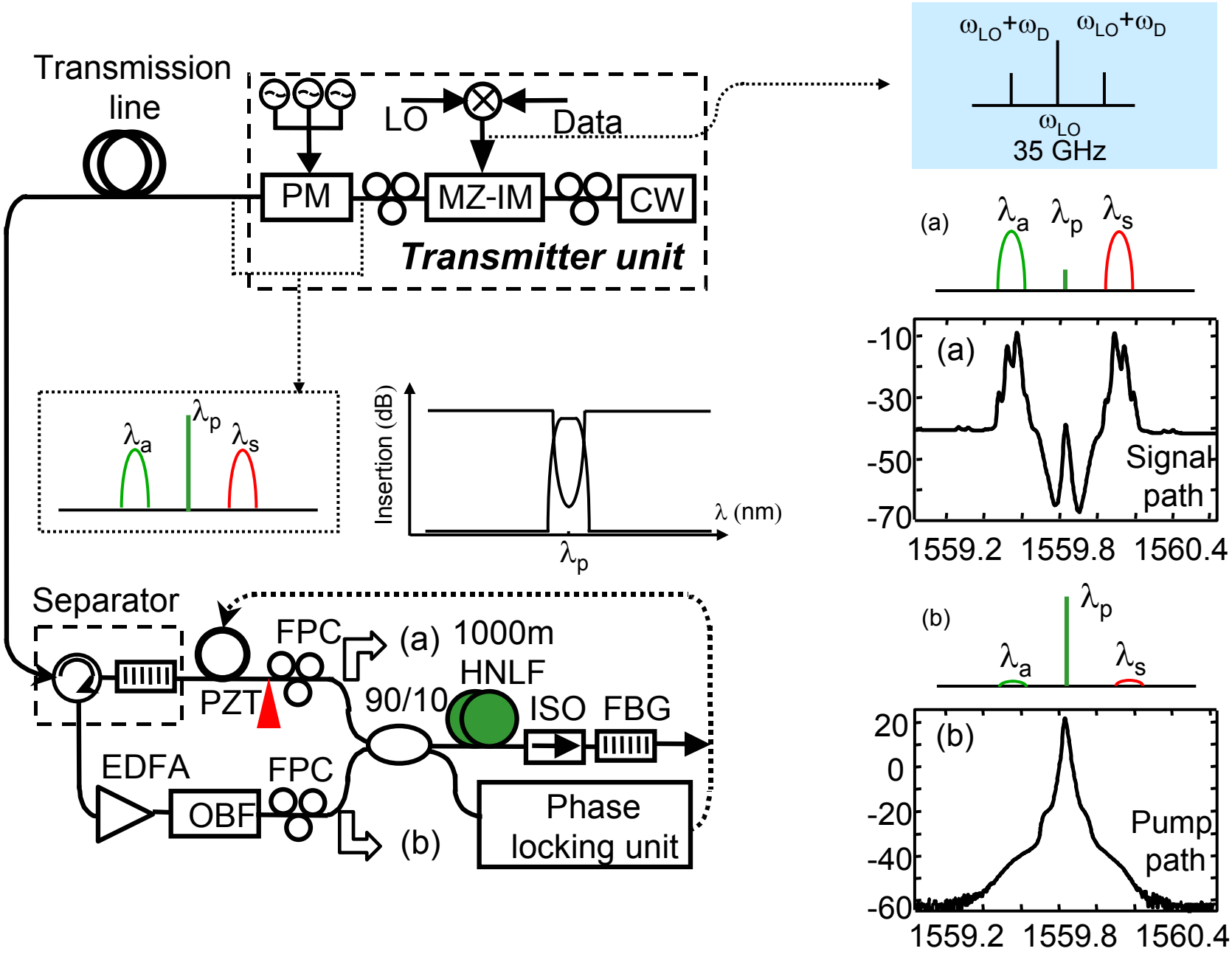

Experimental Results

Output signal vs. Input phase relationship

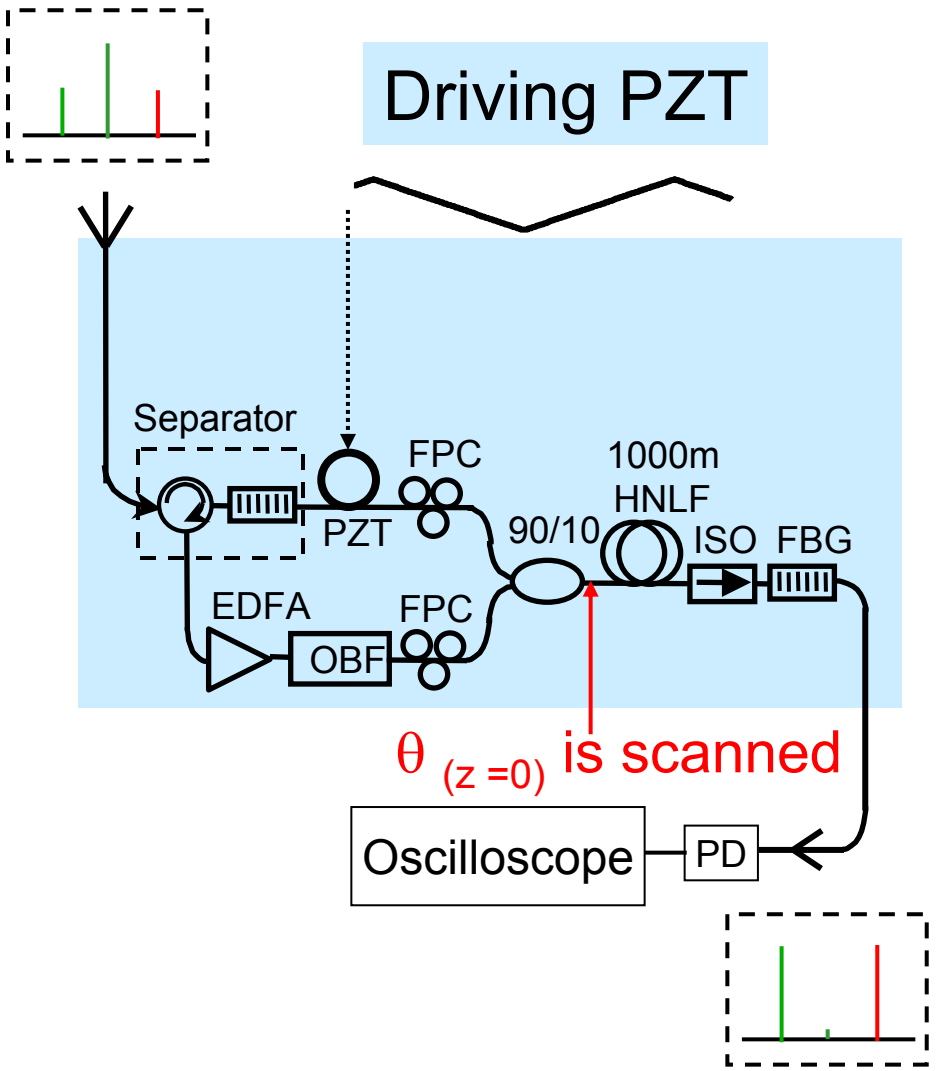

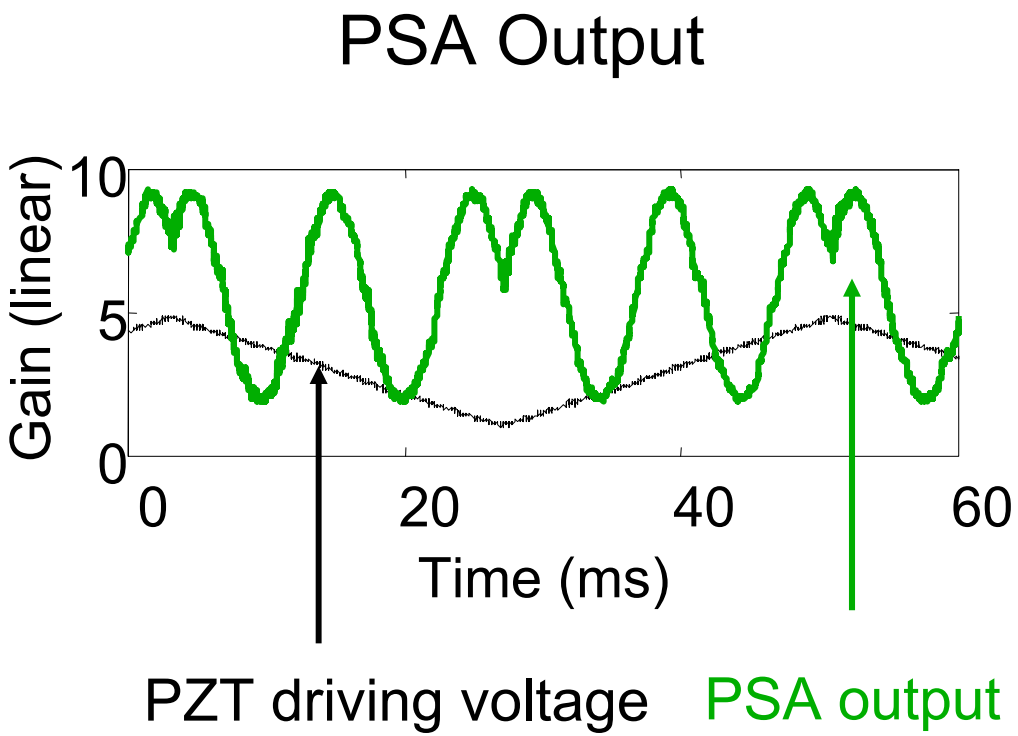

Experimental Results

Amplification & de-amplification

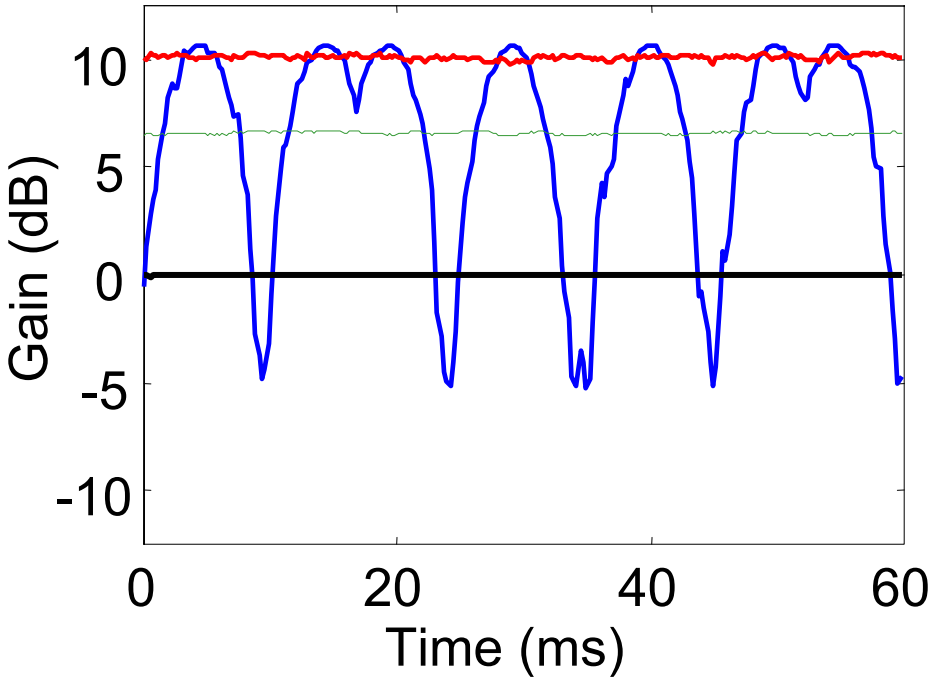

Input signal

Output: phase scanned

Output: phase locked

Output: path-matching broken

Gain vs. Pump Power

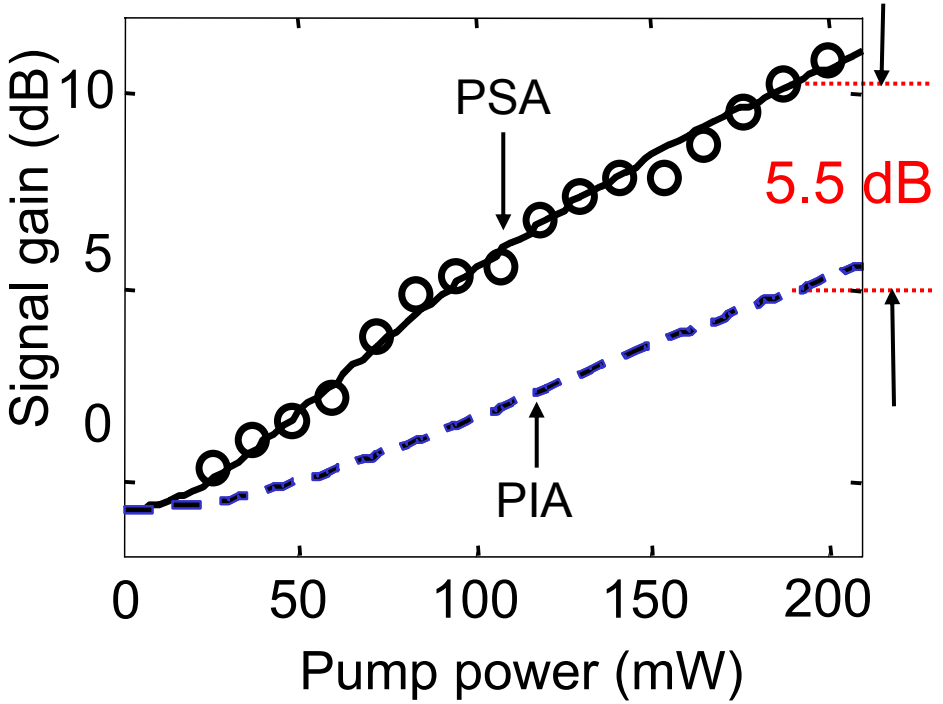

measured PSA gain

calculated PSA gain

calculated PIA gain

Comparison of Theory and Experiment

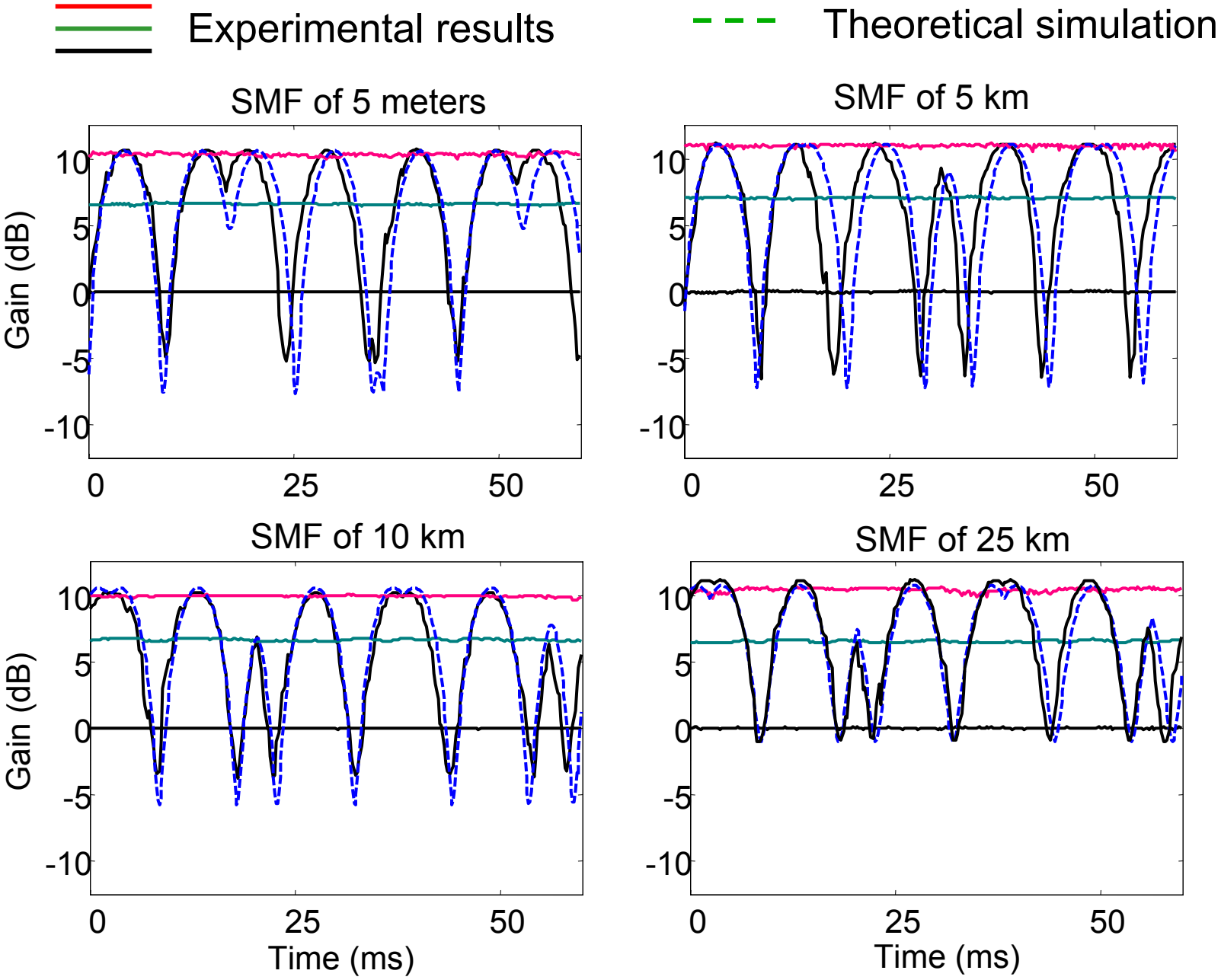

Bit-Error Rate Measurements

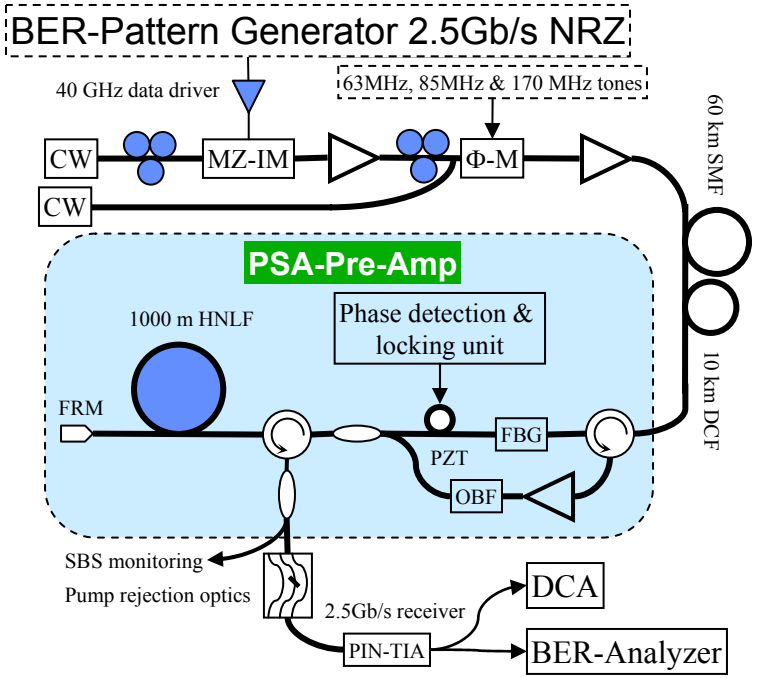

DCF: dispersion compensation fiber
TIA: trans-impedance amplifier
DCA: digital communication analyzer
FBG: fiber Bragg grating

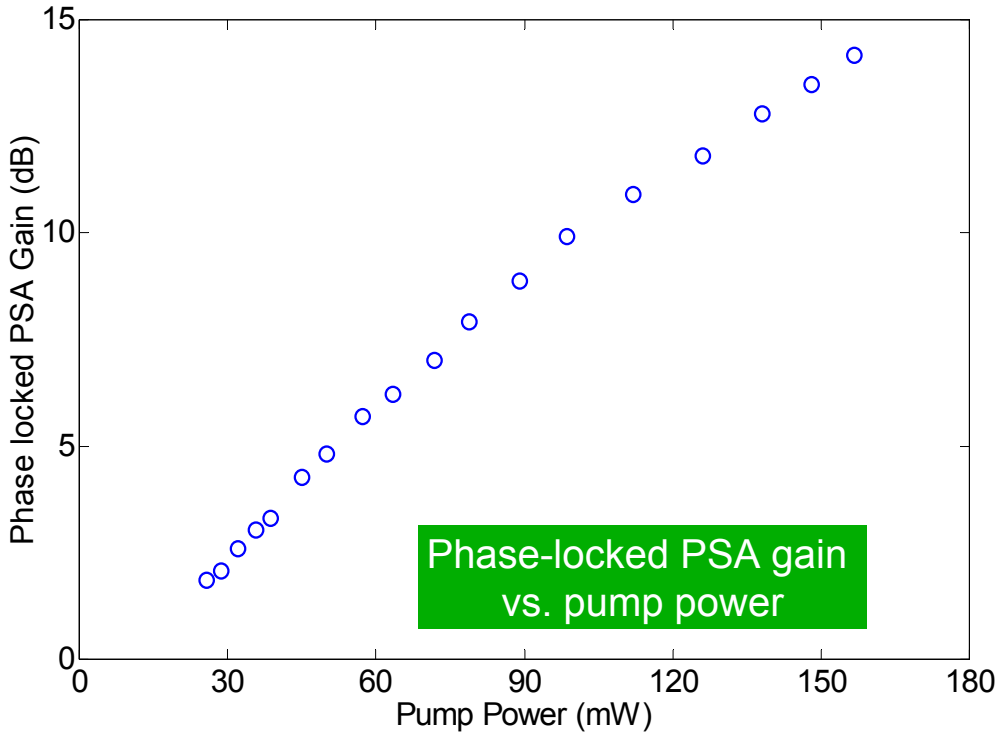

BER Test of the In-Line PS-FOPA

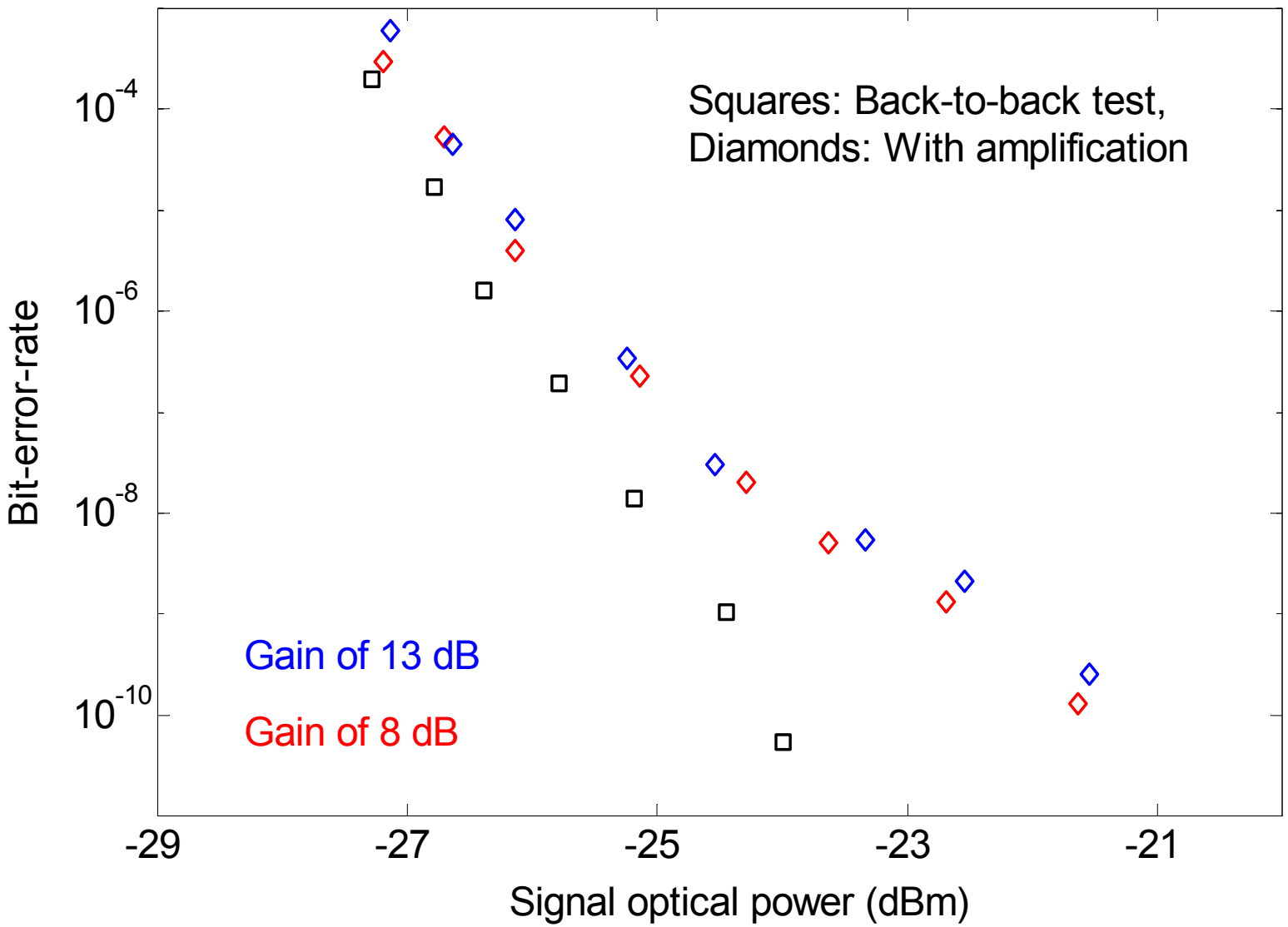

BER Test of Corresponding PI-FOPA

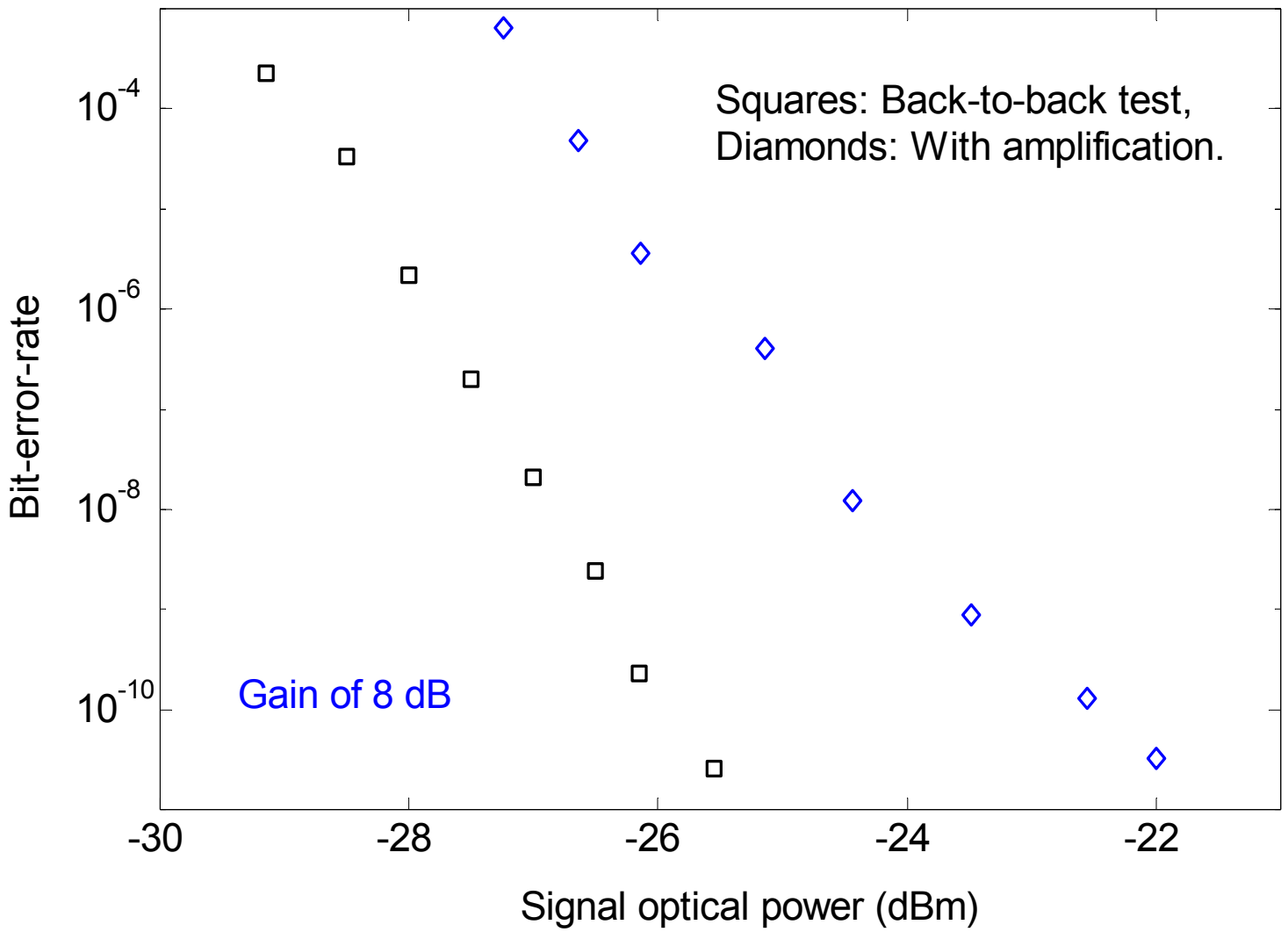

Quantum Laser Radar

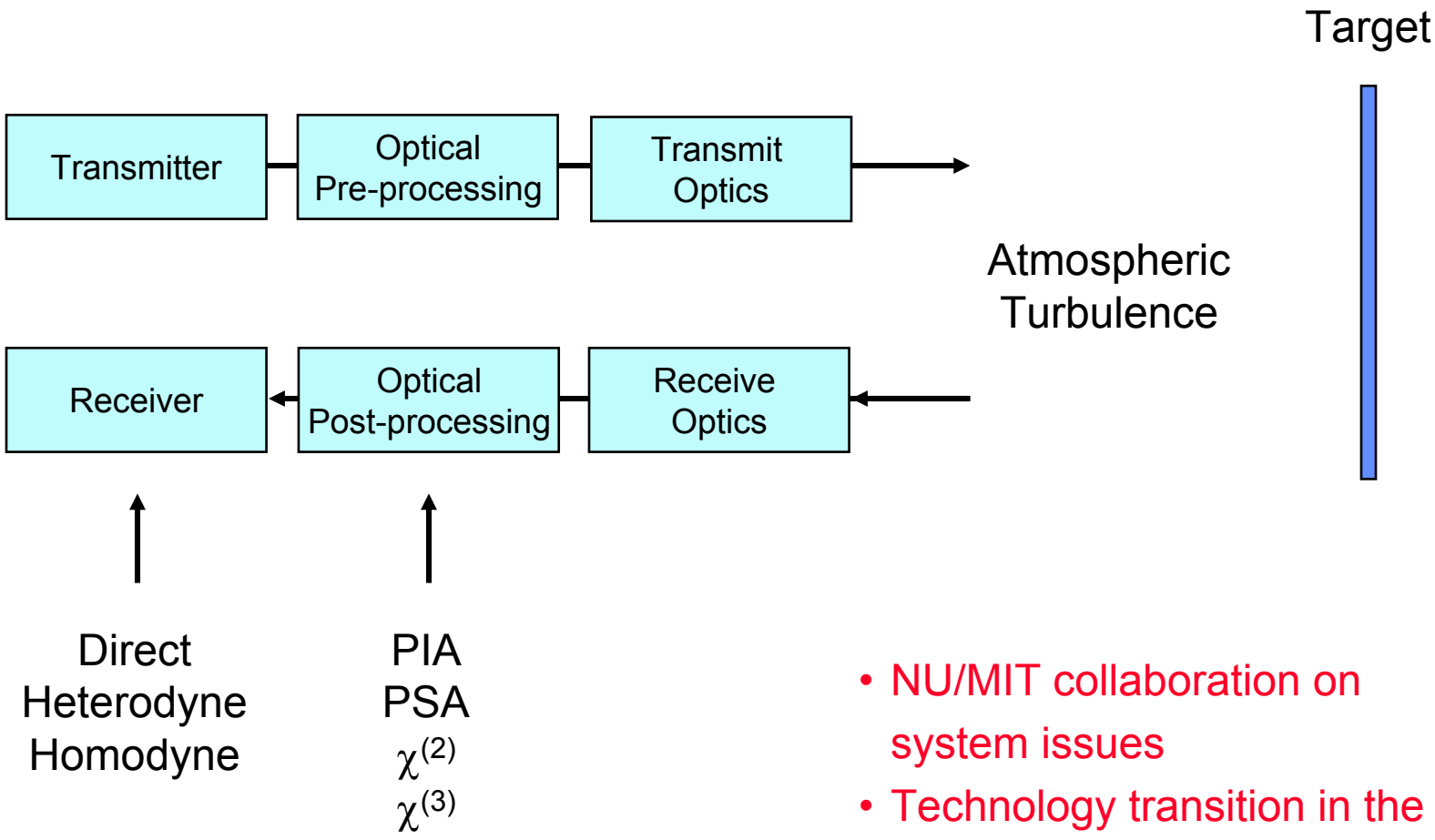

- NU/MIT collaboration on system issues
- Technology transition in the out years of the MURI

Portable Photon-Pair Source: 1st Version

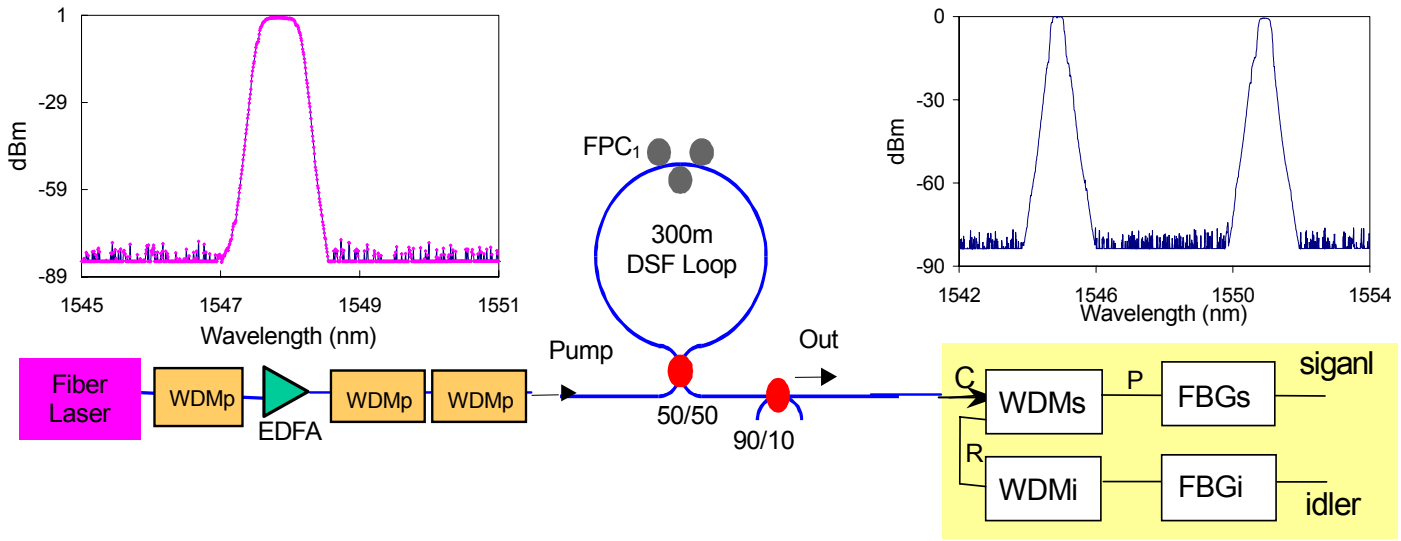

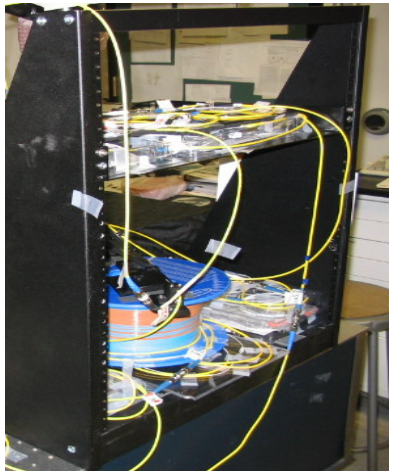

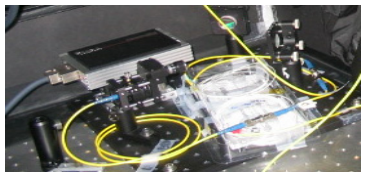

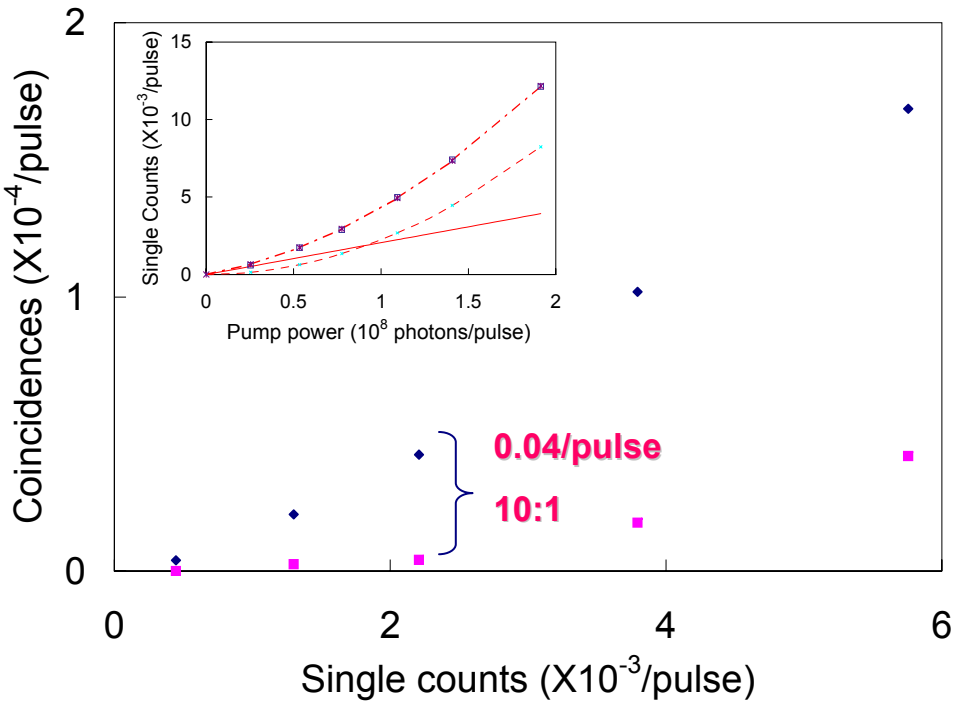

Parameters:

- $\lambda_0 = 1548 \pm 2$nm;
- $\lambda_P = 1547.9$nm,
  1dB bandwidth = 0.45nm,
  FWHM = 0.55nm;
- $\lambda_S = 1550.9$ nm, $\lambda_I = 1544.9$nm,
  1dB bandwidth = 0.3nm,
  FWHM = 0.35nm;
- Efficiency: $\eta_S \approx 7\%$, $\eta_I \approx 7\%$
- Repetition rate: 50 MHz

Northwestern Team's SOW

Quantum Laser Radar: (System)

We will develop quantum imaging techniques specially suited to enhancing the sensitivity and resolution of laser radar. Specific topics to be studied include the use of phase-sensitive amplification as a noiseless preamplification process for enhancing the sensitivity of radar receivers and the use of specially prepared illumination schemes that will enhance system sensitivity. All measurements will be quantified in a manner that allows characterization of the systems aspects of laser radar. (Collaboration with MIT)

Entanglement Utilizing Complex Pump Mode Patterns: (Technology)

We will develop a source of entangled photons based on the orbital angular momentum of light. We will measure and quantify the degree of spatial correlation of this entangled state of light. We will develop new methods to measure the orbital angular momentum of the entangled photons and quantum imaging applications including a quantum motion sensor. (Collaboration with University of Rochester)

Properties of Spontaneous Parametric Down Conversion

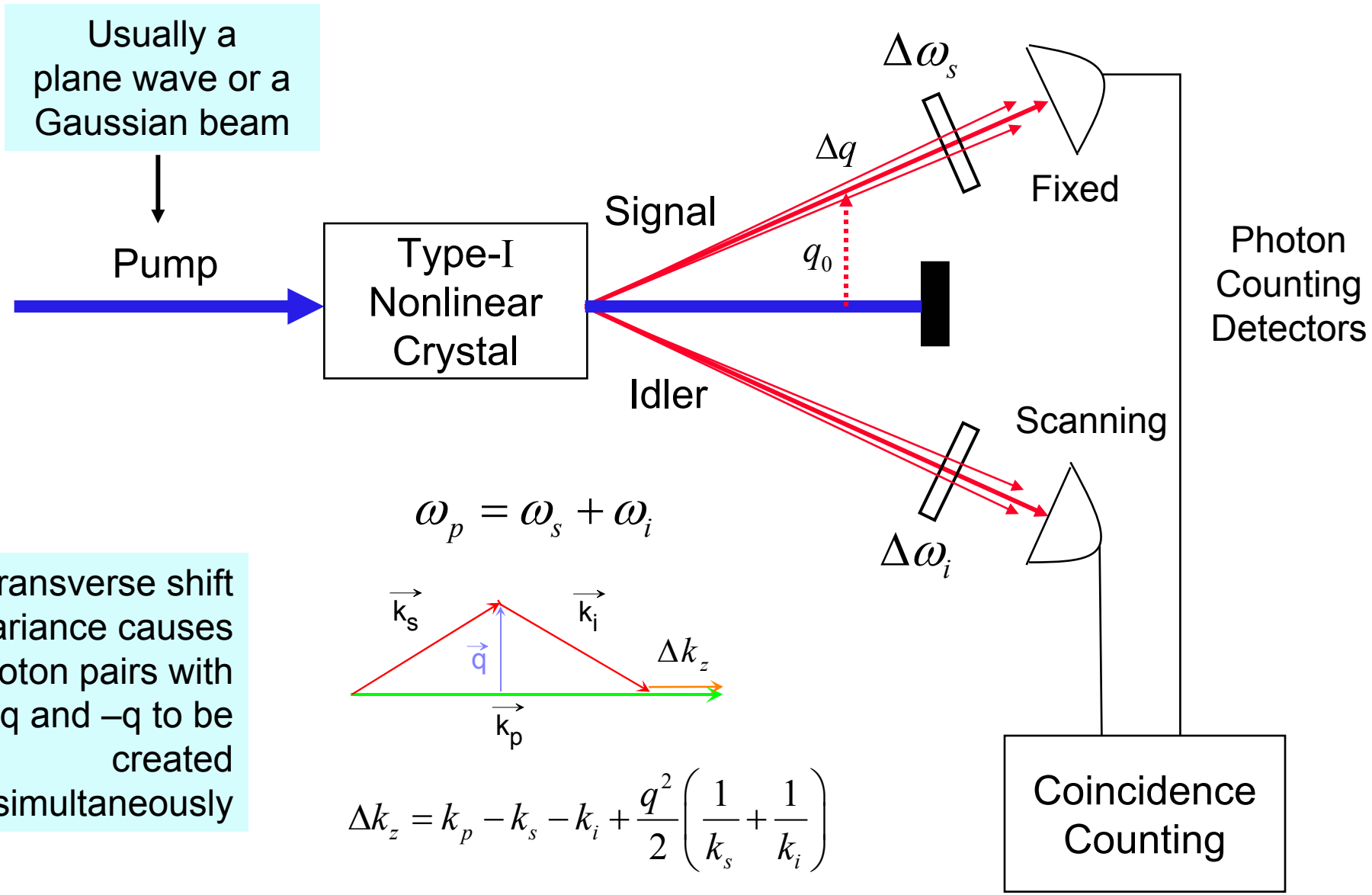

Properties of Spontaneous Parametric Down Conversion

- Photons are created in pairs.
- Photon pairs produce a cone at the output.
- The angle of the cone is determined by the phase matching condition inside the nonlinear crystal.
- Filters should be placed in front of the detectors to select photons at the desired wavelength.
- When pump is a plane wave (k_p is definite), pump, signal, and idler wavevectors are in the same plane.
- Coincidence counts recorded by the scanning detector constitutes a pattern that is dependent on the pump.

Geometry at the Detection Plane

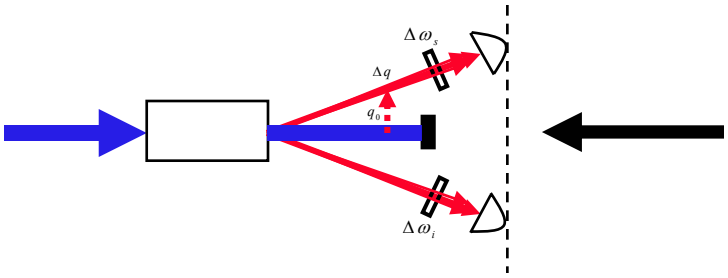

$\Delta k_z = 0$

Δk_y

Δk_x

pump

$\Delta\mathbf{k}=0$

fixed detector

scanned area

Our Motivation

Parametric down conversion with generalized pumps

- In particular, pumps carrying orbital angular momentum
  - Arnaut and Barbosa, PRL **85**, 286 (2001)
- Manifestation of conservation of OAM in parametric down conversion
  - Mair, Vaziri, Weihs, and Zeilinger, Nature **412**, 313 (2001)
- Coincident spot is predicted to be split, another manifestation of OAM
  - Barbosa, Euro Phys. Jour. D **22**, 433 (2003)
- *We have demonstrated this feature for the first time*

Experimental Setup

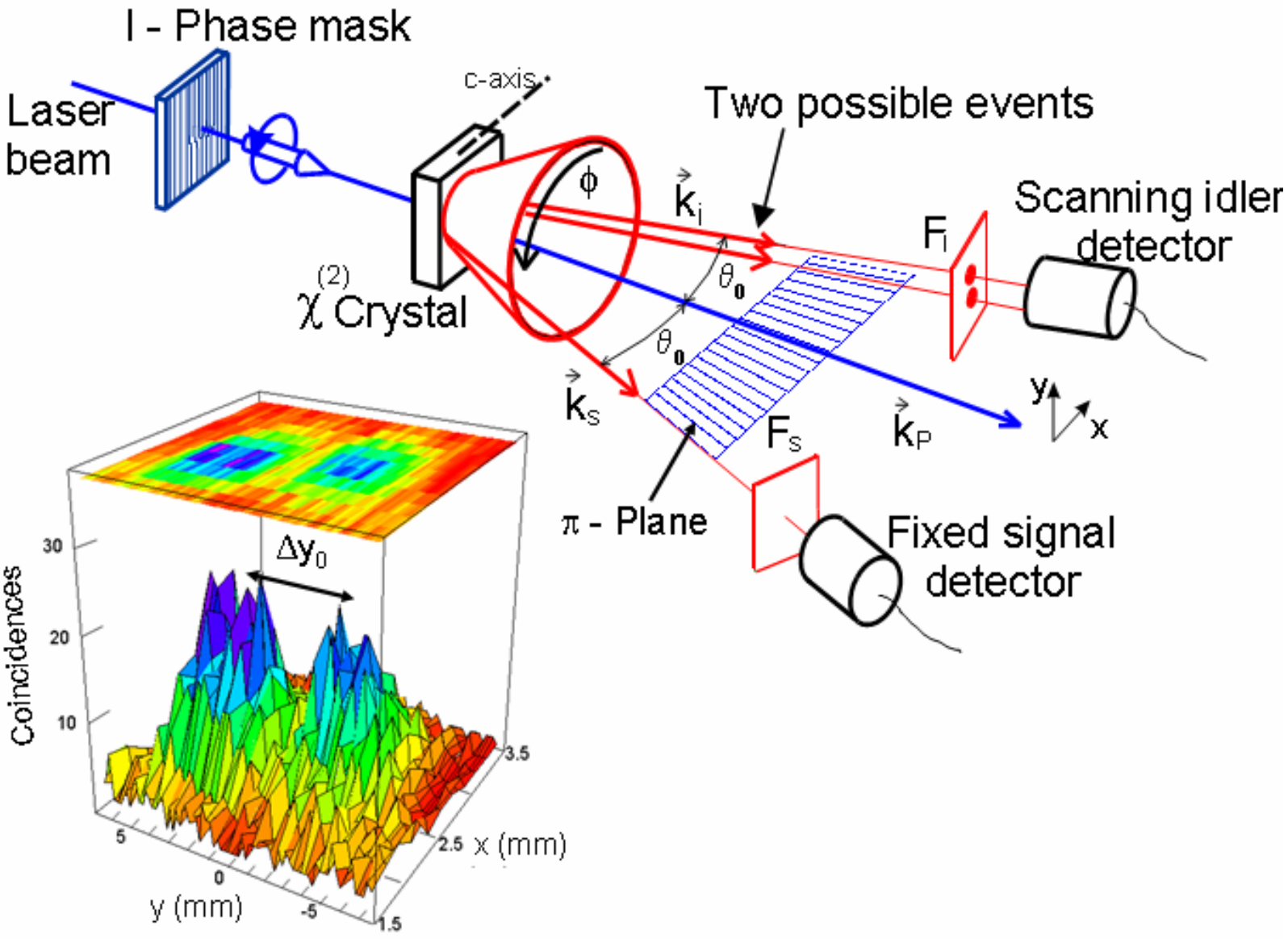

Details of Experimental Parameters

- Pump: CW Argon laser (λ_p = 351.1nm)
- Nonlinear crystal: Type-I BBO ($\theta = 35.2^o$, $\phi = 90^o$)
- Pump beam is focused with a f = 17.5cm lens.
- Filters: 10nm bandwidth interference filters (λ = 702nm) are used with the detectors.
- Single photon counting modules (SPCMs):
  - Detector area of 175μm×175μm
  - Dark counts < 25/s.
- Distance between the detectors and BBO is 30cm.
- No optics between the detectors and BBO.

Gaussian Pump ($l = 0$)

Single Counts

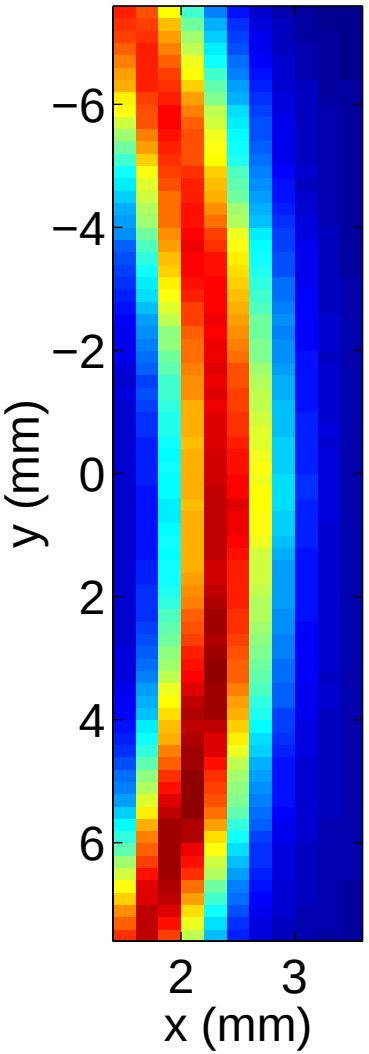

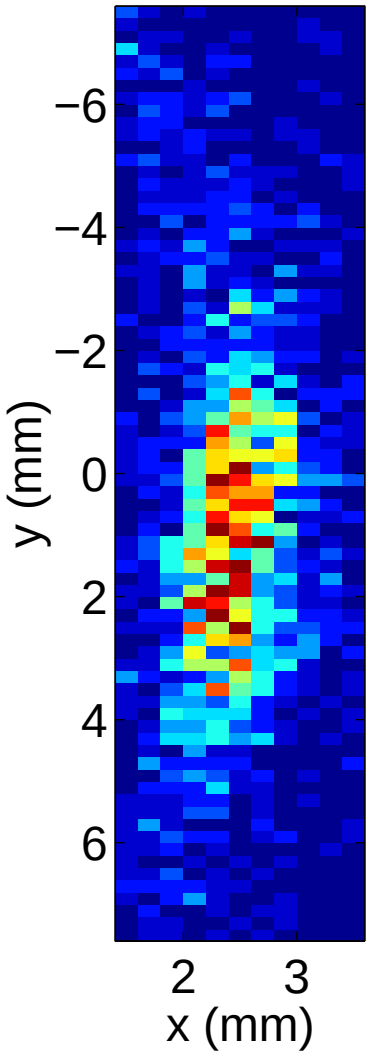

Coincidence Counts

Pump with *l* = 4

Single Counts

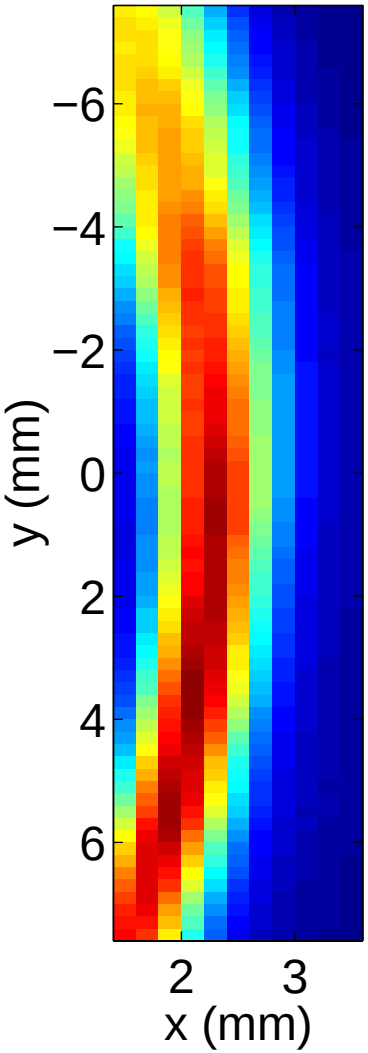

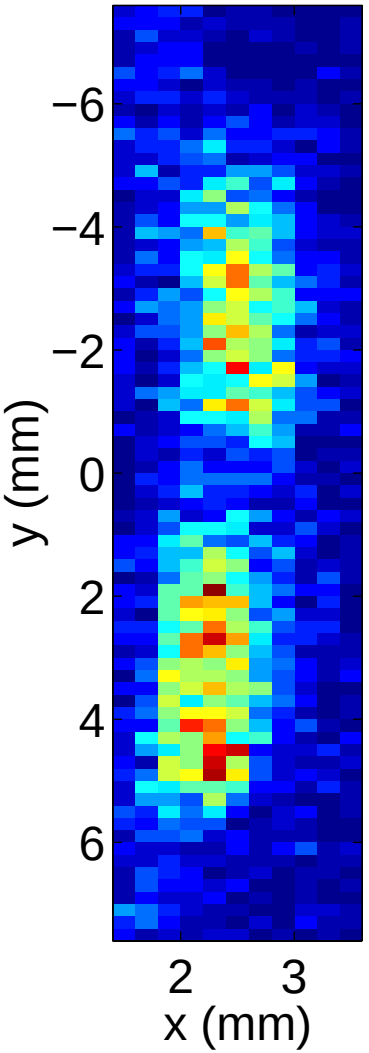

Coincidence Counts

Down-Converted Quantum State

Low gain degenerate case $(\lambda_s = \lambda_i = 2\lambda_p)$

$$|\psi\rangle = |0\rangle + F(\Delta\mathbf{k})\hat{a}^\dagger(\mathbf{k_s})\hat{a}^\dagger(\mathbf{k_i})|0\rangle$$

$$\begin{aligned} \Delta\mathbf{k} &= \mathbf{k}_p + \mathbf{k}_s - \mathbf{k}_p \\ F(\Delta\mathbf{k}) &\propto \int d^3r \;\; \psi_{pl}(\mathbf{r}) \times \exp(-i\Delta\mathbf{k}\cdot\mathbf{r}) \end{aligned}$$

Under the assumption of weak focusing

$$\begin{aligned} F(\Delta\mathbf{k}) \propto & \int dz \exp(-i\Delta k_z) \\ & \times \int dxdy \;\; \psi_{pl}(x,y) \exp(-i[\Delta k_x x + \Delta k_y y]) \end{aligned}$$

Coincidence Pattern

- $F(\Delta\mathbf{k})$ is the product of
  - Axial phase-mismatch term: Determines the spatial bandwidth of the system. A ring shaped pattern the center of which is determined by the pump.
  - Transverse phase-mismatch term: The Fourier transform of the pump on $(\Delta k_x, \Delta k_y)$ coordinate system.
- Fourier transform of the pump is transferred to the coincidence pattern.
- Complex patterns may be observed using different pump beams.
- Pump with angular momentum: Fourier transform of a Laguerre-Gaussian is also a Laguerre-Gaussian.

Predicted Coincidence Pattern for a Pump with OAM

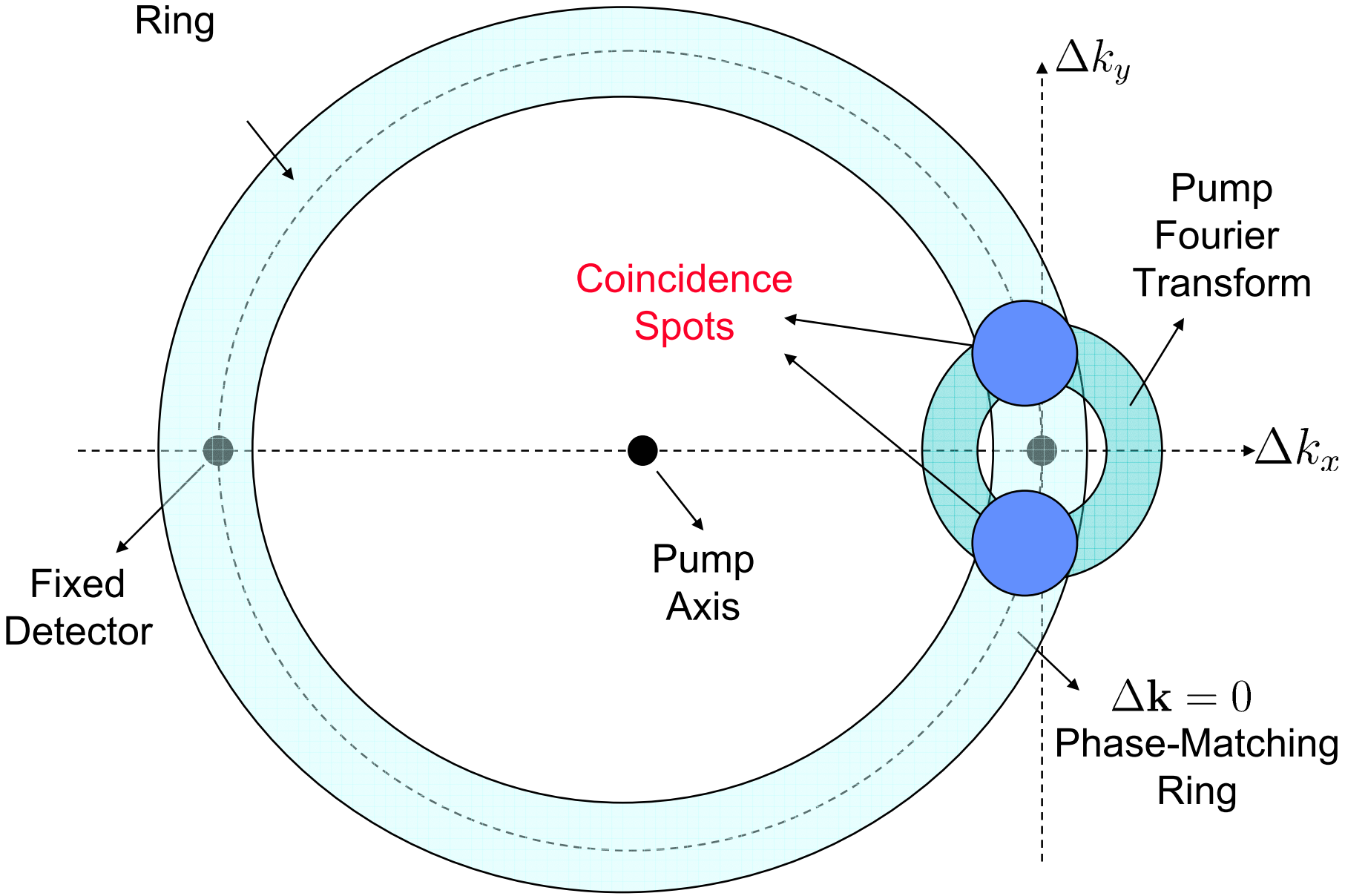

Classical or Quantum?

- Quantum Picture: Coincidence events cannot happen at the same time (no triple counts)
- Semi-classical Picture: Coincidence spots are generated independently. Triple counts may occur.
- GRIN lenses followed by fiber coupled SPCMs are used to measure the triple counts.
- Counts are recorded over 10^4 seconds.

Measurement of the Triple Counts

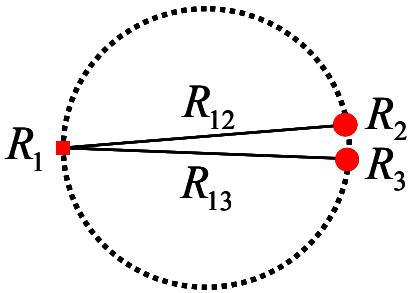

(a)

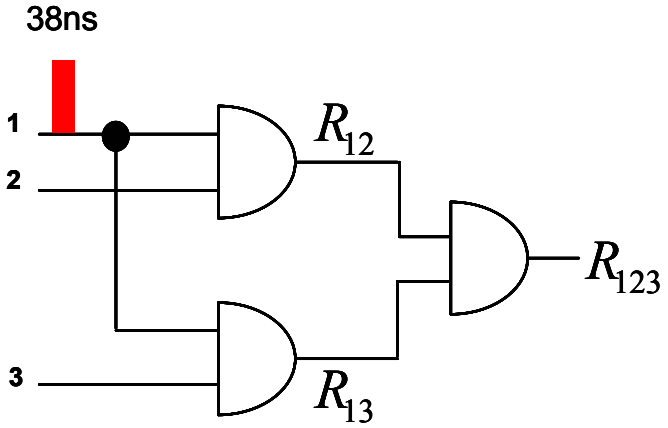

(b)

Triple count rate for semi-classical case

$$R_{123} = \frac{R_{12}R_{13}}{R_1} = 0.0211/sec$$

Results

R_1	564/s
R_2	21479/s
R_3	22486/s
R_{12}	4.1/s
R_{13}	2.9/s
R_{123}	0.0076/s

Future Work: Quantum Imaging with an Arbitrary Pump

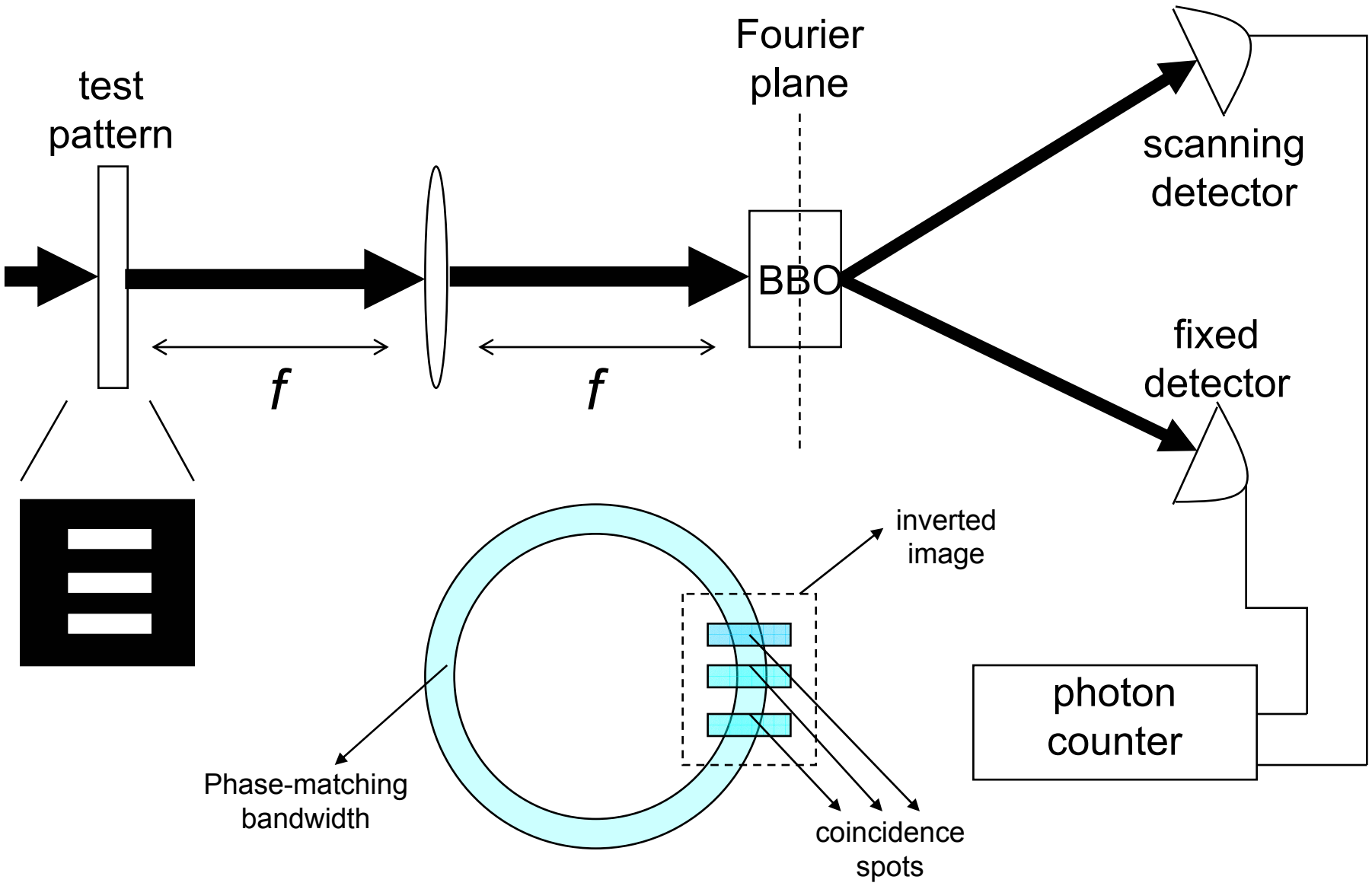

Experimental Results

Single Counts

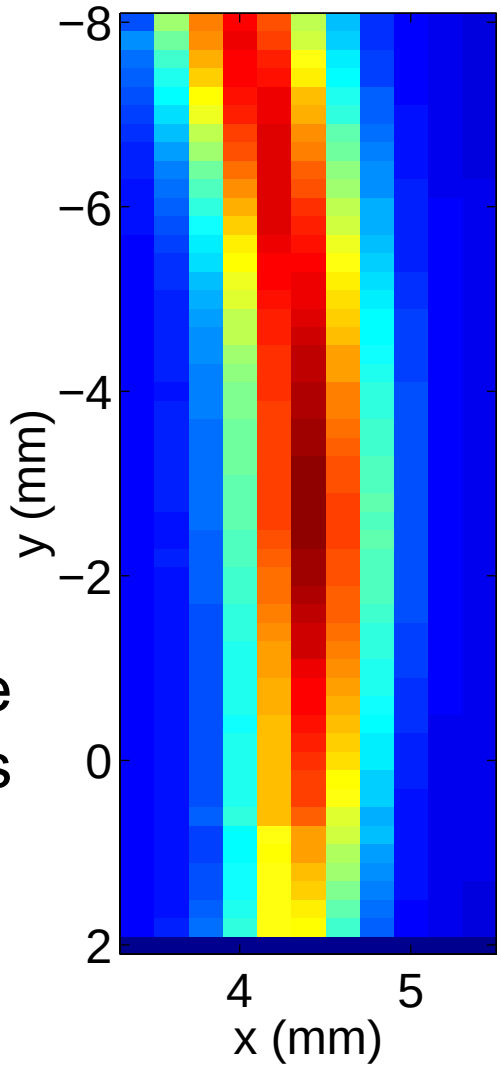

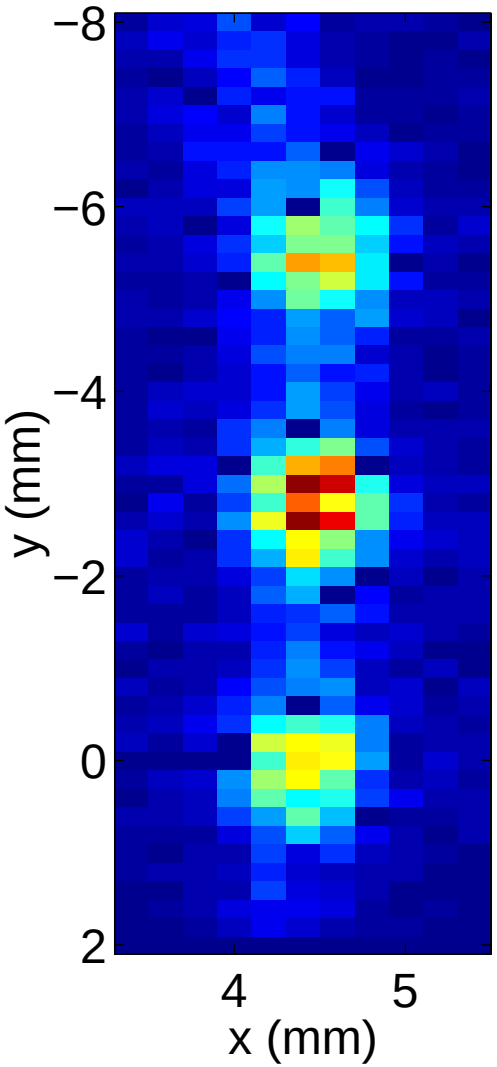

Coincidence Counts

Measurement of Triple Counts

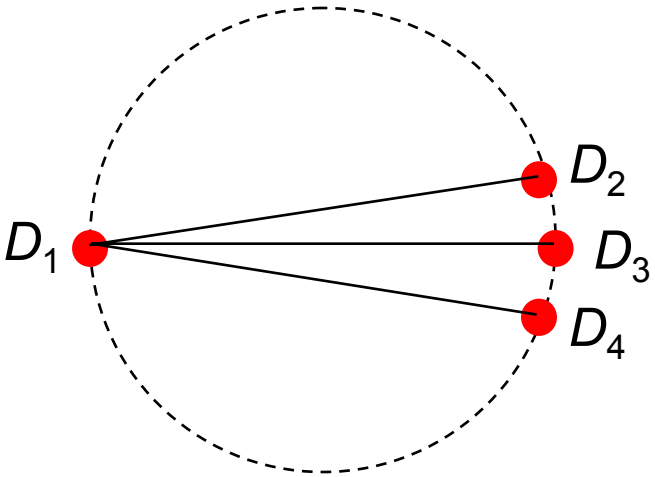

2-4	3-4	2-3
R_1=1350/s	R_1=1201/s	R_1=1062/s
R_2=41981/s	R_3=15539/s	R_2=11494/s
R_4=55030/s	R_4=13393/s	R_3=14594/s
R_{12}=22.25/s	R_{13}=7.547/s	R_{12}=5.797/s
R_{14}=18.74/s	R_{14}=4.263/s	R_{13}=7.36/s
R_{124}=0.1038/s	R_{134}=0.0078/s	R_{123}=0.0087/s

Triple-count rates for semi-classical case

R_{124} = 0.3088/s R_{134} = 0.0268/s R_{123}=0.0402/s

Applications

Generation of Multimode Entangled States

- The coincidence events are exclusive.
- The output may be represented by the following entangled quantum state:

$$|\psi\rangle = |1\rangle_1 \frac{X|1\rangle_2|0\rangle_3|0\rangle_4 + Y|0\rangle_2|1\rangle_3|0\rangle_4 + Z|0\rangle_2|0\rangle_3|1\rangle_4}{\sqrt{|X|^2 + |Y|^2 + |Z|^2}}$$

- 1 denotes spatial mode covered by the fixed detector.
- 2,3,4 denote orthonormal modes, one each for coincidence spots.

Measurement of orbital angular momentum l

Replace (pair of) holographic masks or Dove sorters

$l = 0, 1, 2, 3$

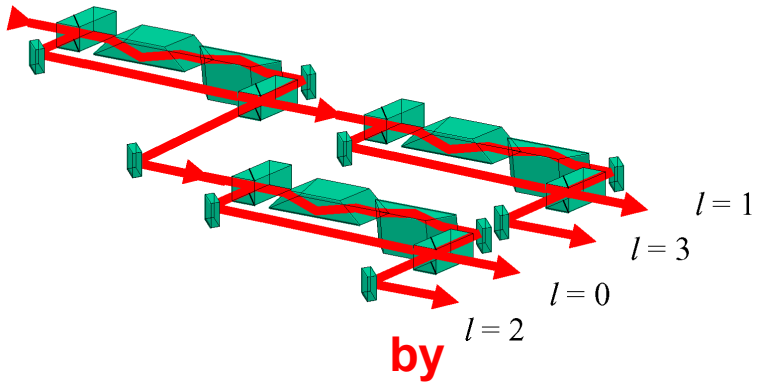

by

Dove sorters are cumbersome, e.g.

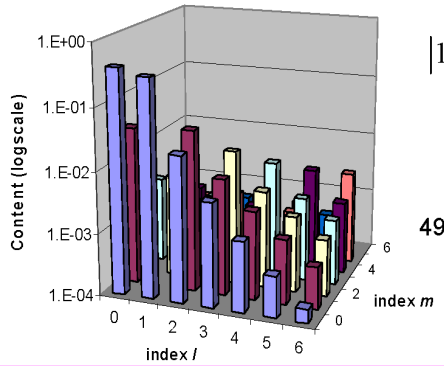

$$|1/2\rangle = \sum_{l=-\infty,\, p=0}^{\infty} \langle l, p|1/2\rangle |l, p\rangle$$

49 LG-modes → 90% fidelity

Spatial multiple coincidence detection for constant of motion measurement

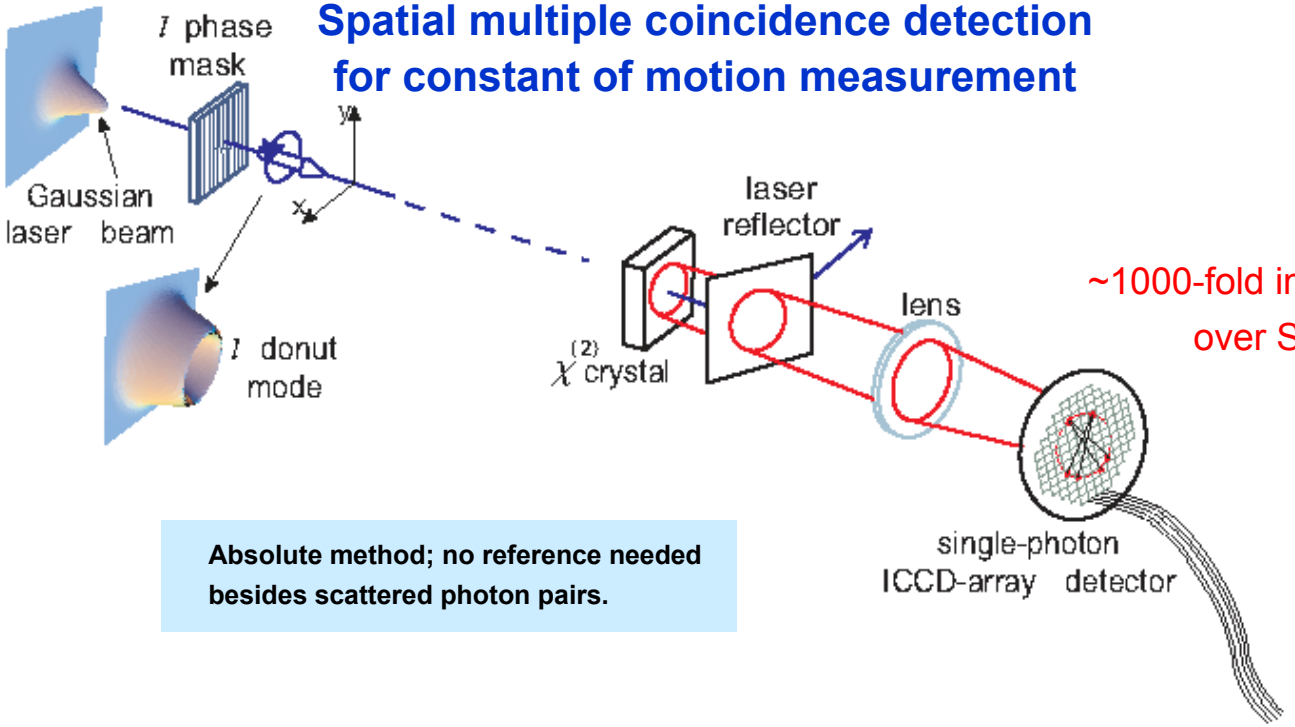

~1000-fold improvement over SCPM

Absolute method; no reference needed besides scattered photon pairs.

Applications: Quantum computation elements

Theoretical study of specific processors and experimental development of components needed

Proposal: Quantum Calculator (Half Adder)

Step-by-step physical implementation for a quantum half-adder using entanglement with **orbital angular momentum** states

(Barbosa, 2005 – MURI&NSF)

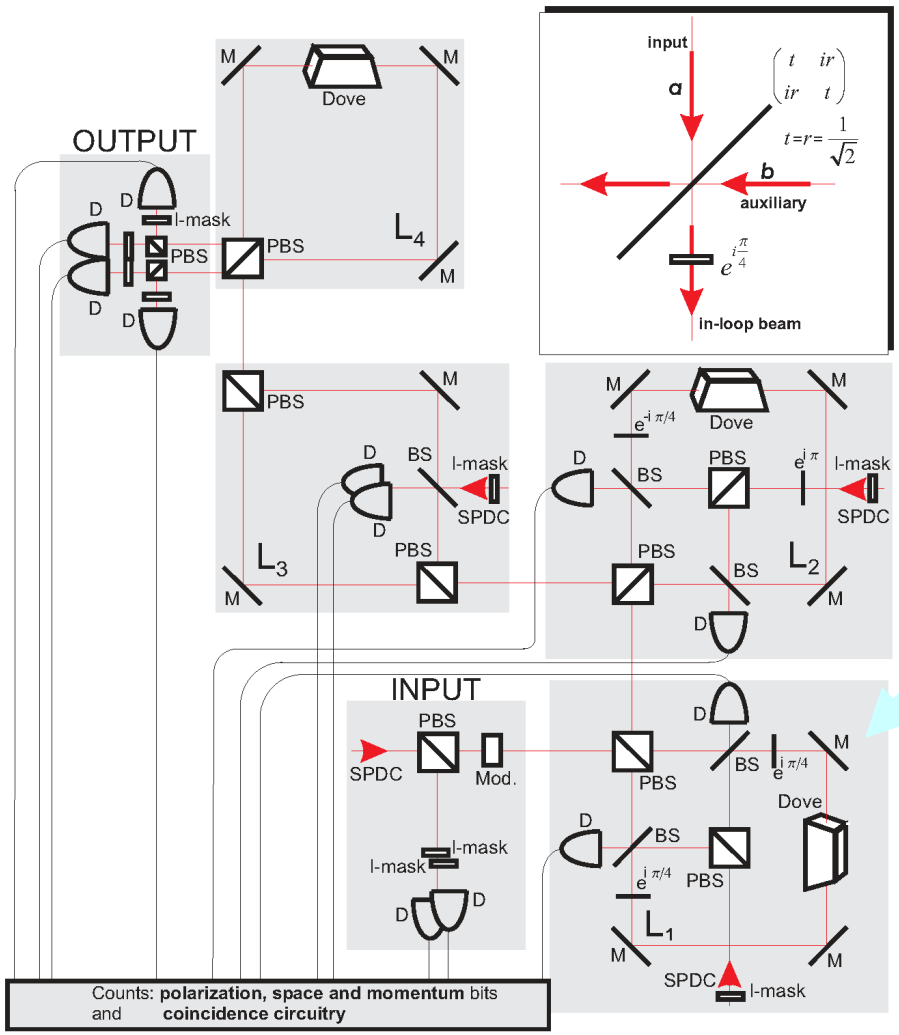

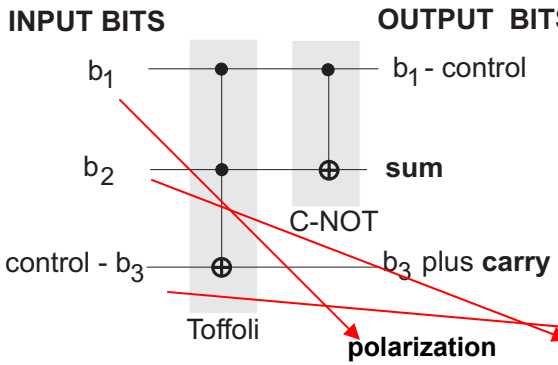

b_1	b_2	sum	carry
1	1	0	1
1	0	1	0
0	1	1	0
0	0	0	0

polarization space angular momentum

$$|\psi_{in}\rangle \Rightarrow \psi(psm)_{in} = \begin{pmatrix} 1-p \\ p \end{pmatrix} \otimes \begin{pmatrix} 1-s \\ s \end{pmatrix} \otimes \begin{pmatrix} 1-m \\ m \end{pmatrix}$$

Loop example: Loop 1

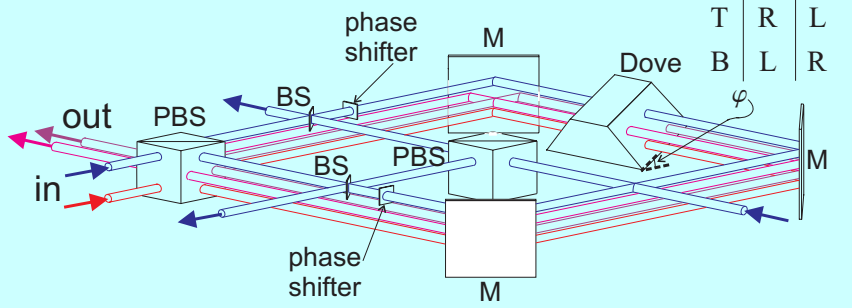

	H	V
T	R	L
B	L	R

$$\psi(p_o s_o m_o)_{out} = \begin{pmatrix} 1-p_o \\ p_o \end{pmatrix} \otimes \begin{pmatrix} 1-s_o \\ s_o \end{pmatrix} \otimes \begin{pmatrix} 1-m_o \\ m_o \end{pmatrix},$$

$$\text{where } p_o = p, s_o = p+s-2ps, m_o = ps+m-2psm.$$

Fulfills truth table

Applications: Motion detection

Theoretical study of OAM field transformations between two coordinate frames and **estimates for motion detection using OAM entangled photon pairs:**

1) **Field transformations**
2) **Parametric Down Conversion with transformed fields**

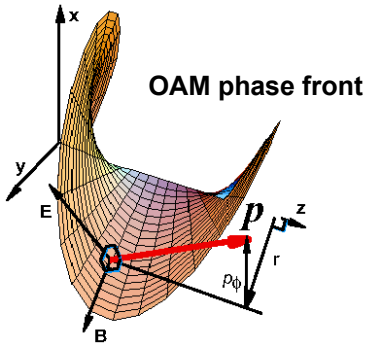

OAM phase front

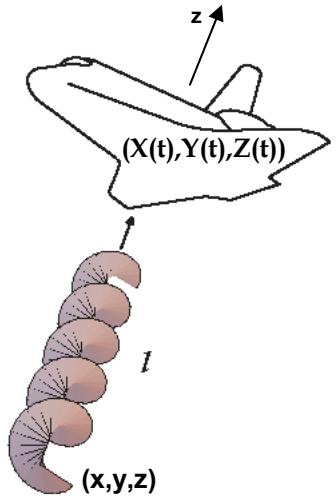

Uniformly rotating frame

For 1) see, for example: Electromagnetic Waves in a Rotating Frame of Reference
J. C. Hauck and **B. Mashhoon,** arXiv:gr-qc/0304069 v2 18 Jun 2003

Some Experimental Challenges

- **Bright source of entangled photons (Multiple photon pairs)**

Generation of ultrabright tunable polarization entanglement without spatial, spectral, or temporal constraints
M. Fiorentino, G. Messin, C. E. Kuklewicz, F. N. C. Wong, and J. H. Shapiro, Phys. Rev. A **69**, 041801 (2004).
Bright, single-spatial-mode source of frequency non-degenerate,polarization-entangled photon pairs using periodically poled KTP
M. Pelton, P. Marsden, D. Ljunggren, M. Tengner, A. Karlsson, A. Fragemann, C. Canalias, F.Laurell, Opt. Express **15**, 3573 (2004).
Observation of Four-Photon Interference with a Beam Splitter by Pulsed Parametric Down-Conversion
Z. Y. Ou, J.-K. Rhee, and L. J. Wang2, PRL **83**, 959 (1999)
Pulsed Twin Beams of Light
O. Aytür and P. Kumar, PRL **65**, 1551 (1990)

welcome joint effort within MURI

- **ICCD arrays and coincidence electronics**

welcome joint effort within MURI

- **Fabrication and testing of OAM masks and axicons for scattered light**

Micromachined brass molds and polymer deposition

welcome joint effort within MURI

- **1 post-doc and 1 graduate student**

- **Possibly, extra support source needed for completion of "Quantum calculator" project.**